NUMERICAL PREDICTION OF FORCED CONVECTION AND PRESSURE DROP CHARACTERISTICS FOR TURBULENT FLOW OF Al_2O_3/WATER NANOFLUID IN A CIRCULAR PIPE

by

Deniz Filiz

M.S., Mechanical Engineering, Boğaziçi University, 2017

Submitted to the Institute for Graduate Studies in
Science and Engineering in partial fulfillment of
the requirements for the degree of
Master of Science

Graduate Program in Mechanical Engineering
Boğaziçi University

2017

ACKNOWLEDGEMENTS

I would first like to thank my thesis advisor Prof. Dr. Kunt Atalık of the Mechanical Engineering Faculty at Boğaziçi University. The door of Prof. Atalık's office was always open whenever I ran into a trouble spot or had a question about my research or writing.

I must express my very profound gratitude to my parents, especially my sister, and to my friends for providing me with unfailing support and continuous encouragement throughout my study and through the process of researching and writing this thesis. This accomplishment would not have been possible without them. Thank you.

ABSTRACT

NUMERICAL PREDICTION OF FORCED CONVECTION AND PRESSURE DROP CHARACTERISTICS FOR TURBULENT FLOW OF Al_2O_3/WATER NANOFLUID IN A CIRCULAR PIPE

Fully developed turbulent forced convection flow of an Al_2O_3/water nanofluid in a circular pipe under constant wall heat flux is investigated numerically, using finite volume method. Both single phase model and two phase models such as mixture and Eulerian are considered. Different correlations for nanofluids thermophysical properties have been compared in the single phase formulation to investigate the Brownian effect for both turbulent and laminar flow. The results given by the single phase and two phase models are compared to the experimental results in the literature. The heat transfer enhancement and the increase in the pressure drop of the nanofluid are found to be more significant when the Reynolds number and/or the volume concentration are increased in accordance to experimental results. The single phase model is observed to give accurate predictions when direct correlations for nanofluid properties are available from experimental data. The predictions given by the two phase Eulerian model are more accurate for dilute suspensions at low volume concentrations, however for higher concentrations, the two phase mixture model gives closer results to experimental data, when compared to the Eulerian model. It is also found that Brownian motion is effective in heat transfer enhancement for both laminar and turbulent flow of nanofluids. The heat transfer enhancement increases with increasing Reynolds number and volume concentration, while the pressure drop increase depends only on volume concentration. For both low and high volume concentrations, the heat transfer enhancement to pressure drop increase ratio is observed to be higher in the turbulent case compared to laminar flow.

ÖZET

DAİRESEL BORU İÇİNDEKİ Al_2O_3/SU NANOAKIŞKANININ TÜRBÜLANSLI AKIŞ VE ISI TRANSFER KARAKTERİSTİKLERİNİN SAYISAL OLARAK İMCELENMESİ

Sabit duvar ısı akısı altındaki bir dairesel boruda Al_2O_3/su nanoakışkanın tam gelişmiş türbülanslı zorlanmış taşınım akış problemi, sonlu hacim yöntemi kullanılarak sayısal olarak incelenmiştir. Hem tek fazlı model hem de karışım ve Eulerian gibi iki faz modeller denenmiştir. Hem türbülanslı ve hem de laminer akışta Brownian etkisi araştırmasında nanoakışkanların termofiziksel özellikleri için farklı korelasyonlar, tek fazlı formülasyon kullanılarak karşılaştırılmıştır. Tek fazlı ve iki fazlı modellerin sonuçları literatürdeki deneysel sonuçlar ile karşılaştırılmıştır. Modelleme ile, deney sonuçlarında da görüldüğü gibi, Reynolds sayısı ve / veya hacimsel konsantrasyonu arttırıldığında ısı transferindeki ve basınç düşüşündeki artışın daha belirgin olduğu bulunmuştur. Tek fazlı modelin, nanoakışkan özellik-leri için deneysel verilerden doğrudan korelasyonlar elde edildiğinde daha doğru sonuçlar verdiği gözlemlenmiştir. İki fazlı Eulerian modeli ile bulunan sonuçlar, düşük hacimsel konsantrasyonlarında seyreltik süspansiyonlar için daha doğru; ancak daha yüksek konsantrasyonlar için, iki fazlı karışım modelinin, deney sonuç-larına göre Eulerian modelinden daha yakın sonuç verdiği görülmüştür. Brownian hareketinin hem laminer hem de türbülanslı akış için ısı transferi artışında etkili olduğu bulunmuştur. Isı transferi artışı, artan Reynolds sayısı ve hacimsel konsantrasyonu ile birlikte artarken, basınç düşüşü artışı sadece hacimsel konsantrasyonuna bağlıdır. Düşük ve yüksek hacimsel konsantrasyonları için, laminar akışa kıyasla türbülanslı durumda ısı transferindeki artışın basınç düşüşündeki artışa oranının daha yüksek olduğu gözlemlenmiştir.

TABLE OF CONTENTS

ACKNOWLEDGEMENTS . . . iii
ABSTRACT . . . iv
ÖZET . . . v
LIST OF FIGURES . . . viii
LIST OF TABLES . . . x
LIST OF SYMBOLS . . . xii
LIST OF ACRONYMS/ABBREVIATIONS . . . xiv
1. INTRODUCTION . . . 1
1.1. Research Background . . . 1
1.2. The Objectives of the Present Work . . . 2
1.3. Scope and Limitations . . . 3
2. LITERATURE REVIEW . . . 5
2.1. Thermophysical Properties of Nanofluids . . . 5
2.1.1. The Effective Thermal Conductivity . . . 5
2.1.2. The Effective Viscosity . . . 10
2.2. Studies About Forced Convective Heat Transfer of Nanofluids . . . 14
2.2.1. Experimental Studies . . . 15
2.2.2. Numerical Studies . . . 22
2.2.2.1. The single phase model . . . 23
2.2.2.2. The two phase models . . . 26
2.3. Research Gaps . . . 29
3. MODELLING OF THE FORCED CONVECTION OF NANOFLUIDS . . . 32
3.1. Introduction . . . 32
3.2. Basic Definitions About Flow and Heat Transfer . . . 33
3.2.1. Flow Analysis . . . 33
3.2.2. Thermal Analysis . . . 35
3.3. Methodology . . . 37
3.3.1. Geometry and Boundary Conditions . . . 37
3.3.2. Thermophysical Properties of The Nanofluid . . . 37

3.3.3. Governing Equations 41
3.3.3.1. Single Phase Formulation 41
3.3.3.2. Two Phase Formulation 42
3.3.4. Turbulence Modelling 45
3.3.5. Numerical Method and Validation 46
3.4. Results and Discussions 50
3.4.1. Flow Model Comparison for Different Volume Concentration Values 50
3.4.2. Comparison of Brownian Motion Effects on the Heat Transfer Enhancement for Laminar and Turbulent Flows 57
3.4.3. Comparison of Pressure Drop Estimations for Laminar and Turbulent Flow of Nanofluid 61
3.4.4. Comparison of Some Flow and Thermal Parameters for Turbulent Al_2O_3 /water Nanofluid Flow 62
3.4.5. Comparison of Heat Transfer Enhancement and Pressure Drop Increase for Laminar and Turbulent Al_2O_3/water Nanofluid Flow 64
3.4.6. Comparison of Simulation results of Turbulent Al_2O_3/water Nanofluid Flow with Proposed Correlations and Chilton-Colburn Analogy . 68
4. CONCLUSION AND FUTURE WORK 71
4.1. Conclusion 71
4.2. Contribution and Future Work 73
REFERENCES 75
APPENDIX A: UDF CODES 86
A.1. Sample UDF Code (Patel *et al.*'s Model) 86
A.2. Sample UDF Code (Chon *et al.*'s Model) 88

LIST OF FIGURES

Figure 3.1. The geometry of the flow problem. 38

Figure 3.2. The final mesh structure of Domain 2. 48

Figure 3.3. The velocity (left) and temperature (right) contours of water flow at Re=30000. 49

Figure 3.4. The Nusselt number (left) and the friction factor (right) comparison of water simulation for Domain 2. 50

Figure 3.5. The Nusselt number comparison of dilute Al_2O_3/water nanofluid for different flow models ($\emptyset$ =0.03% (top left), $\emptyset$ =0.054% (top right), $\emptyset$ =0.135% (bottom)). 51

Figure 3.6. The Nusselt number comparison of dilute CuO/water nanofluid for different flow models ($\emptyset$ =0.015% (top left), $\emptyset$ =0.118% (top right), $\emptyset$ =0.236% (bottom)). 52

Figure 3.7. The Nusselt number comparison of Al_2O_3/water nanofluid for different flow models ($\emptyset$ =1.8% (left) and $\emptyset$ =3.6% (right)). 53

Figure 3.8. The local heat transfer coefficient at x=1 m comparison for different property models ($\emptyset$ =1.32% (left) and $\emptyset$ =2.76% (right)). 58

Figure 3.9. The average heat transfer coefficient comparison for different property models ($\emptyset$ =1.8% (left) and $\emptyset$ =3.6% (right)). 58

Figure 3.10. The wall temperature changes along the pipe wall for $\emptyset$ =0%, $\emptyset$ =1.8% and $\emptyset$ =3.6% cases at Re=15000. 63

Figure 3.11. The maximum velocity changes along the pipe axis for $\emptyset$ =0%, $\emptyset$ =1.8% and $\emptyset$ =3.6% cases at Re=15000. 63

Figure 3.12. The ratio of convective heat transfer coefficient enhancement of Al_2O_3/water nanofluid for laminar (left) and turbulent (right) flow conditions. 65

Figure 3.13. The ratio of pressure drop increase of Al_2O_3/water nanofluid for laminar (left) and turbulent (right) flow conditions. 66

Figure 3.14. Comparison of the Nusselt number results with existing correlations for nanofluids at $\emptyset$ =1.8% (left) and $\emptyset$ =3.6% (right) volume concentration. 69

LIST OF TABLES

Table 1.1. Thermal conductivities of some materials 2

Table 3.1. The mesh independency test for fully developed turbulent water flow at Re=30000 48

Table 3.2. The Nusselt number percentage error values of dilute $(\emptyset < 0.5\%)$ Al_2O_3/water nanofluid simulations for different flow models 55

Table 3.3. The Nusselt number percentage error values of dilute $(\emptyset < 0.5\%)$ CuO/water nanofluid simulations for different flow models 56

Table 3.4. The Nusselt number percentage error values of $(\emptyset > 1\%)$ Al_2O_3/ water nanofluid simulations for different flow models 56

Table 3.5. The average heat transfer coefficient percentage error values of different thermal conductivity models for Experiment 2 60

Table 3.6. The local heat transfer coefficient percentage error values of different thermal conductivity models for Experiment 3 60

Table 3.7. The pressure drop values and the friction factor comparison for turbulent Al_2O_3/water nanofluid flow 61

Table 3.8. The pressure drop values and the friction factor comparison for laminar Al_2O_3/water nanofluid flow 62

Table 3.9. The ratio of convective heat transfer coefficient enhancement to pressure drop increase comparison of laminar Al_2O_3/water nanofluid flow 67

Table 3.10. The ratio of convective heat transfer coefficient enhancement to pressure drop increase comparison of turbulent Al_2O_3/water nanofluid flow 68

Table 3.11. Chilton-Colburn Analogy for Al_2O_3/water nanofluid 70

LIST OF SYMBOLS

a	Acceleration (m/s^2)
c_p	Specific heat $(\frac{J}{kgK})$
D	Tube diameter (m)
d_p	Particle diameter (m)
f	Friction factor
f_{drag}	Drag function
F_d	Drag force (N)
F_{vm}	Virtual mass force (N)
F_{col}	Particle-particle interaction force (N)
h	Heat transfer coefficient $(W/m^2.K)$
h_v	Volumetric heat transfer coefficient $(W/m^3.K)$
h_p	Liquid-particle heat transfer coefficient $(W/m^2.K)$
k	Thermal conductivity $(\frac{W}{mK})$
K	Turbulent kinetic energy $(\frac{m^2}{s^2})$
K_B	Boltzman constant
L	Length (m)
$Nu = \frac{hD}{k}$	Nusselt number
p	Pressure (Pa)
$Pe = \frac{vD}{\propto_{nf}}$	Peclet number
$Pr = \frac{c_p \mu}{k}$	Prandtl number
q	Wall heat flux $(\frac{W}{m^2})$
$Re = \frac{\rho v D}{\mu}$	Reynolds number
$St = \frac{Nu}{RePr}$	Stanton number
T	Temperature (K)
T'	Fluctuating temperature (K)
V	Velocity vector
v	Velocity $(\frac{m}{s})$
V'	Fluctuating velocity (m/s)

x, y	2-D axisymmetric coordinates (m)
$\alpha = \frac{k}{\rho c_p}$	Thermal diffusivity $(\frac{m^2}{s})$
β	Friction coefficient $(kg/m^3 s)$
γ	Mean free path of water molecule (nm)
ε	Dissipation of turbulent kinetic energy $(\frac{m^2}{s^3})$
μ	Dynamic viscosity $(Pa\ s)$
ρ	Density $(\frac{kg}{m^3})$
τ	Stress (Pa)
τ_p	Particle relaxation time (s)
$\emptyset$	Volume concentration

LIST OF ACRONYMS/ABBREVIATIONS

b	Bulk
bf	Base fluid
eff	Effective
in	Inlet
k	Phase number
l	Liquid
m	Mixture
nf	Nanofluid
out	Out
p	Nanoparticle
s	Solid
t	Turbulence

1. INTRODUCTION

1.1. Research Background

The heat transfer process is a main part of energy industry. Therefore, researchers and engineers are constantly trying to increase the efficiency of the heat transfer process due to limited energy resources and fuel prices. There are many methods such as using extended surfaces like fins, application of vibration and usage of micro channels, already in use to increase the efficiency. Furthermore, the heat transfer efficiency can be improved by adding small solid particles which have higher thermal conductivity than conventional heat transfer fluids (water, oil, and ethylene glycol mixture). However, some researchers stated that these solid particles can cause blockage of heat transfer channels and erosion in channel walls when added solid particles are in millimeters or micrometers size. With developments in nanotechnology, solid particles that can be produced at nanometer size can solve the mentioned problems. Furthermore, the stability of nanoparticles can easily obtained by using proper dispersants.

Nanofluids are used in many areas such as transportation, refrigeration, cooling process, energy industry etc. In these application fields, the heat transfer process is carried out with heat exchangers, evaporators, condensers etc. The size of the heat transfer device is also very important in terms of the space used by the device and the material used to make the device. Furthermore, the power consumption of the pump used to circulate the working fluid in the heat transfer systems is very critical for the efficiency of the system. The usage of nanofluids is recommended as a solution for all the above mentioned topics. Due to their increased thermal properties, nanofluids increase the efficiency of heat transfer systems which leads to compactness of heat transfer devices and significant reduction in power consumption.

Nanofluids are stable suspensions of nanometer sized (<100 nm) metallic and non-metallic particles dispersed in base fluids like water, oil or ethylene glycol. It is highly desirable that the nanoparticles should have high thermal conductivity. There-

fore, Al_2O_3, CuO, TiO_2, Ag, Cu and Fe are frequently used as a nanoparticles. The comparison between thermal conductivities of base fluids and solid particles is shown in Table 1.1. Although spherical particles are commonly used, rod-shaped, tube-shaped and disk-shaped nanoparticles can also be used in some applications.

Table 1.1. Thermal conductivites of some materials [1].

Material	**Thermal Cond. (W/m.K)**
Cu	401
Ag	429
Al_2O_3	40
Water	0.613
Ethylene glycol	0.253
Engine oil	0.145

1.2. The Objectives of the Present Work

In recent period, a lot of researchers have focused on nanofluid due to their remarkable thermal properties. This situation creates many debates among researchers. Therefore, reliable numerical process for flow and heat transfer properties of nanofluids is required for the efficient and sustainable industrial application. Although there are many studies about forced convection of nanofluids, researchers cannot reach a common idea to model nanofluid properties and flow. Therefore, there is need of a universal flow and property models for different volume concentration and Reynolds number ranges.

The main purpose of this work is to create a numerical procedure that will determine the flow and forced convection heat transfer characteristics of Al_2O_3/water nanofluid under turbulent flow condition in a circular pipe. Because the numerical simulation process removes the need of experiments that will be done for different geometries and nanofluids. Furthermore, this work tries to reveal the effect of Brownian motion on heat transfer enhancement for both laminar and turbulent flows comparing

different thermophysical models for nanofluid properties. Moreover, numerical method that gives the right results is investigated in this study without knowing the nanofluid effective thermal properties by using two phase model for different volume concentration and Reynolds number.

For this purpose of the study, the commercial computational fluid dynamics (CFD) tool ANSYS Fluent is used. Pure water flow inside smooth tube is used for validation of code and four different experimental works which have wide range of volume concentration including dilute case and Reynolds number are used to test the numerical procedure by using two dimensional single phase and two phase models.

1.3. Scope and Limitations

The scope of this study is limited to forced convection heat transfer of the Al_2O_3/water nanofluid inside a circular pipe under laminar and turbulent flow. Because these conditions are valid for many heat transfer applications. This study can be selected as a reference study to determine flow and thermophsyical property models of nanofluid for wide range of volume concentration and Reynolds number. Furthermore, this study reveals optimum working condition of nanofluid in heat transfer applications in terms of pressure drop and heat transfer rate. The $k-\varepsilon$ turbulence model is selected since this model is commonly used by other researchers and other turbulence models are not included in the content of this study. Horizontal tubes with diameters ranging from 4.5 to 9.4 mm have been considered according to selected four experimental works. Due to flow symmetry with respect to the tube axis, the half of the flow domain is considered to save computational time. The effect of gravity has been neglected. To investigate the Brownian effect on nanofluid flow and heat transfer, wide range of thermal conductivity models are tested. Since the results of single phase flow model highly depend on the thermal conductivity model, the validity of the property models is checked. Therefore, one can easily choose the property model according to the application range after reading this study. The Reynolds number varies between 400-1900 and 7000-31000 for laminar and turbulent flow respectively. The wall heat flux, the inlet temperature and the inlet mass flow rate are chosen according to consid-

ered experiments. The nanoparticle volume concentrations varies between 0% to 4%. Therefore, this study considers both dilute and high concentration range.

2. LITERATURE REVIEW

2.1. Thermophysical Properties of Nanofluids

Thermophysical properties of the nanofluids are very important since their enhanced heat transfer behavior strongly depends on them. Especially, the viscosity and the thermal conductivty of base fluid increase when the nanoparticles are added. Therefore, many researchers tried to understand the reason of such enhancement. They explained that the effective thermal conductivity and viscosity may depend on many parameters such as volume concentration, nanoparticle and base fluid type, particle size, particle shape, and temperature. Although there are many studies in the literature about thermophysical properties of the nanofluids, the thermophysical property correlations give different results as there is no common idea about the enhancement mechanism of the nanofluids.

2.1.1. The Effective Thermal Conductivity

Although there are many models to predict the effective thermal conductivity of nanofluids, none of them can accurately measure the thermal conductivity of the nanofluid on a wide range of volume concentration, particle size, temperature, etc. All thermal conductivity models can be classified under two group which are static and dynamic models. Static models are earlier models and they are very basic since they only depend on volume concentration and thermal conductivities of base fluid and nanoparticle.

The Maxwell model [2] is the first model proposed for two phase spherical solid particle-liquid mixtures and it is given by

$$k_{eff} = k_{bf}\left(\frac{k_p + 2k_{bf} + 2\left(k_p - k_{bf}\right)\emptyset}{k_p + 2k_{bf} - 2\left(k_p - k_{bf}\right)\emptyset}\right) \tag{2.1}$$

where k_{eff} is the effective thermal conductivity of the mixture, k_{bf} is the thermal conductivity of the base fluid, k_p is the thermal conductivity of the solid particle and $\emptyset$ is the volume concentration. This model predicts the mixture thermal conductivity at low volume concentrations and ambient conditions. The Maxwell model is the basis for the static models that are subsequently proposed.

Some researchers have taken into account some factors related to the nanofluids and they improved the Maxwell model. One of these models is Hamilton and Crosser model [3] and it is given by

$$k_{eff} = k_{bf}\left(\frac{k_p + (n-1)k_{bf} - (n-1)\left(k_{bf} - k_p\right)\emptyset}{k_p + (n-1)\,k_{bf} + \left(k_{bf} - k_p\right)\emptyset}\right) \tag{2.2}$$

where the empirical shape factor, n, is taken $3/\Psi$. Ψ is the sphericity and it means the ratio of the surface are of a sphere with volume equivalent to that of the average particle, to the surface area of the particle. It has numerical value according to particle shape.

Yu and Choi [4] said that these two model predicts the mixture thermal conductivity for volume concentration up to 1%. Therefore, they improved the Maxwell model by considering effect of interfacial nanolayers. Their model is described as

$$k_{eff} = k_{bf}\left(\frac{k_p + 2k_{bf} + 2\left(k_p - k_{bf}\right)(1+\beta)^3\emptyset}{k_p + 2k_{bf} - \left(k_p - k_{bf}\right)(1+\beta)^3\emptyset}\right) \tag{2.3}$$

where β is the ratio of the nanolayer thickness to the diameter of the nanoparticle.

The classical static models compute the thermal conductivity of the nanofluid roughly and they are often unreliable since they do not consider the effect of important parameters such as the particle size, the clustering effect, the Brownian motion and temperature. It is found by some researchers that the thermal conductivity of the nanofluid increases with decreasing nanoparticle size due to liquid layering around nanoparticles and the Brownian motion.

There are some dynamic models that considers some important parameters about the nanofluids in the literature.

Koo and Kleinstreuer [5] developed a model that includes both static and dynamic part. They used the Maxwell model as a static part and add the Brownian motion term into their correlation. The model considers the effects of particle size, temperature, volume concentration and the Brownian motion and the model is described by

$$k_{eff}=k_{static}+k_{brownian} \tag{2.4}$$

$$k_{brownian}= 5.10^4\beta\emptyset\rho_{bf}c_{p,bf}\sqrt{\frac{K_BT}{\rho_p d_p}}f(T,\emptyset) \tag{2.5}$$

where β is the fraction of the liquid volume which travels with a particle, K_B is the Boltzman constant, T is temperature and d_p is the particle size. They described β and $f(T,\emptyset)$ with some correlations by using experimental data and these correlations varied with different nanofluid type. Koo and Kleinstreuer' s correlation is valid in the range of $1\% < \emptyset < 4\%$ and $300\ K < T < 325\ K$.

Chon *et al.* [6] reported an experimental correlation which describes the thermal conductivity of Al_2O_3 nanofluids. They stated that the Brownian motion is a key mechanism of heat transfer enhancement and their correlation depends on the Brownian motion effect. Their correlation is given by

$$\frac{k_{eff}}{k_{bf}}= 1 + 64.7\emptyset^{0.746}\left(\frac{d_{bf}}{d_p}\right)^{0.369}\left(\frac{k_p}{k_{bf}}\right)^{0.7476} Re_p^{1.2325} Pr_{bf}^{0.9958} \tag{2.6}$$

where Pr_{bf} is the Prandtl number of the base fluid and given by

$$Pr_{bf}=\frac{c_{p,bf}\mu_{bf}}{k_{bf}} \tag{2.7}$$

and Re_p is the particle Reynolds number and described by

$$Re_p = \frac{\rho_{bf} K_B T}{3\pi \mu_{bf}^2 \gamma} \tag{2.8}$$

and γ is the mean free path of base fluid molecule. The model is applicable for $1\% < \emptyset < 4\%$ and $21°\text{C} < T < 71°\text{C}$.

Patel *et al.* [7] found that the reasons behind the heat transfer enhancement of nanofluid are increase in the surface area and the Brownian motion effect through micro-convection. Their correlation is described as

$$\frac{k_{eff}}{k_{bf}} = 1 + \frac{d_{bf}}{d_p} \frac{\emptyset}{1-\emptyset} \frac{k_p}{k_{bf}} (1 + 25000\ Pe) \tag{2.9}$$

where Pe is Peclet number and described as

$$Pe = \frac{2K_B T}{\pi \mu_{bf} d_p^2} \frac{d_p}{\propto_{bf}} \tag{2.10}$$

It is applicable for $1\% < \emptyset < 8\%$ and $20°C < T < 50°C$.

Jang and Choi [8] investigated the thermal conductivity enhancement mechanism of nanofluids and they found that four modes which are the heat transfer by the base fluid, thermal diffusion of nanoparticles, the Brownian motion which is the result of nanoparticle collision and the nanoconvection which is the result of collision between nanoparticle and base fluid molecules. They developed the correlation by considering these modes and the correlation is described as

$$k_{eff} = k_{bf}\,(1-\emptyset) + 0.01 k_p \emptyset + (18.10^6) \frac{d_{bf}}{d_p} k_{bf} Re_p^2 Pr_{bf} \emptyset \tag{2.11}$$

Li and Peterson [9] investigated the dispersion effect of nanoparticles due to the Brownian motion. They researched velocity, temperature and pressure distribution around the nanoparticles and they found that the Brownian motion is the reason behind the increase in the thermal conductivity. On the contrary, Evans et al. [10] reported that the Brownian motion has a little effect on the thermal conductivity enhancement. They stated that the enhancement highly depends on the clustering effect and interfacial thermal resistance.

There are some semi-empirical correlations which are found by curve-fitting of experimental results.

Maiga *et al.* [11] developed a correlation for Al_2O_3/water nanofluid by using the results of the Hamilton and Crosser [3], Jang and Choi [8] and Chon et al. [6]. They stated that the new correlation considers the Brownian motion effect and can be applicable even for millimeter and micrometer particle size. Their correlation is given by

$$\frac{k_{eff}}{k_{bf}} = 4.97\emptyset^2 + 2.72\emptyset + 1 \tag{2.12}$$

Williams *et al.* [12] developed a correlation by using their experimental result. They proposed two new correlations for Al_2O_3/water and ZrO_2/water nanofluids. The correlations are valid up to 4% volume concentration and are described as

$$\frac{k_{eff}}{k_{bf}} = 1 + 4.5503\emptyset \qquad (for\ Al_2O_3/water) \tag{2.13}$$

$$\frac{k_{eff}}{k_{bf}} = 1 + 2.4505\emptyset - 29.867\emptyset^2 \qquad (for\ ZrO_2/water) \tag{2.14}$$

Mintsa *et al.* [13] investigated thermal conductivities of Al_2O_3 and CuO water nanofluids experimentally. They developed linear correlation that changes with volume concentration and valid within the temperature ranges of 20-50 °C and up to 18%

volume concentration. They stated that particle size, nanoparticle type, volume concentration and bulk temperature of the nanofluid are very important for the effective thermal conductivity. Their correlations are described by

$$\frac{k_{eff}}{k_{bf}} = 1 + 1.72\emptyset \qquad (for\ Al_2O_3/water) \tag{2.15}$$

$$\frac{k_{eff}}{k_{bf}} = 0.99 + 1.74\emptyset \qquad (for\ CuO/water) \tag{2.16}$$

Corcione [14] obtained a new correlation by collecting the experimental data of Al_2O_3, CuO, TiO_2 and Cu nanoparticles dispersed in water or ethylene glycol from various researchers. The correlation is given by

$$\frac{k_{eff}}{k_{bf}} = 1 + 4.4(\frac{\mathrm{T}}{T_{fr}})^{10}(\frac{k_p}{k_{bf}})^{0.03} Re_p^{0.4} Pr_{bf}^{0.66} \tag{2.17}$$

where T_{fr} is the freezing point of the base liquid and

$$Re_p = \frac{2\rho_{bf} K_B T}{\pi \mu_{bf}^2 d_p} \tag{2.18}$$

Most of the published experimental results or correlations are not in agreement with each other and they give different results even for the same base fluid, same nanoparticle, same particle size, same volume concentration and same temperature. Moreover, none of the researchers reach an agreement on the thermal conductivity enhancement mechanism. Therefore, various thermal conductivity models should be investigated to get correct results.

2.1.2. The Effective Viscosity

The number of the studies that investigate the viscosity of nanofluids is less when compared to the articles that investigate the thermal conductivity of nanofluids. This is an expected result since the effect of nanofluids on heat transfer is more important.

However, the viscosity is very important feature that defines flow characteristics. Different models have been proposed by different researchers to determine the effective viscosity of nanofluids and most of them depend on the volume concentration. Firstly, Einstein [15] has defined an equation to obtain the effective viscosity value of spherical solid particle suspensions and it is described by

$$\frac{\mu_{eff}}{\mu_{bf}} = (1 + 2.5\emptyset) \tag{2.19}$$

where μ_{eff} is the effective viscosity of suspension. Generally, this equation is used for dilute nanofluids which have volume concentration less than 0.5%.

Later, Brinkman [16] developed Einstein's equation by extending its volume concentration validity range up to 4%. This equation is expressed as

$$\frac{\mu_{eff}}{\mu_{bf}} = \frac{1}{(1 - \emptyset)^{2.5}} \tag{2.20}$$

Batchelor [17] defined a new equation by considering the effect of the Brownian motion for an isotropic suspension of rigid and spherical particles. The equation is described as

$$\frac{\mu_{eff}}{\mu_{bf}} = 1 + 2.5\emptyset + 6.5\emptyset^2 \tag{2.21}$$

Williams *et al.* [12] developed a correlations for Al_2O_3/water and ZrO_2/water nanofluids by performing curve fitting to their experimental data. The correlations are given by

$$\frac{\mu_{eff}}{\mu_{bf}} = e^{(4.91\emptyset/0.2092-\emptyset)} \qquad (for\ Al_2O_3/water) \tag{2.22}$$

$$\frac{\mu_{eff}}{\mu_{bf}} = 1 + 46.8\emptyset + 550.82\emptyset^2 \qquad (for\ ZrO_2/water) \tag{2.23}$$

which have validity ranges of volume concentration up to 6% and 3%, respectively.

Nguyen *et al.* [18] proposed viscosity correlations of Al_2O_3 (36 nm, 47 nm) and CuO (29 nm) nanoparticles dispersing in water by making exponential and linear assumption at 22°C. Their correlations are valid in the range of $1\% < \emptyset < 13\%$ and are described as

$$\frac{\mu_{eff}}{\mu_{bf}} = 1 + 0.025\emptyset + 0.015\emptyset^2 \qquad (for\ 36\ nm\ Al_2O_3/water) \qquad (2.24)$$

$$\frac{\mu_{eff}}{\mu_{bf}} = 0.904e^{0.148\emptyset} \qquad (for\ 47\ nm\ Al_2O_3/water) \qquad (2.25)$$

$$\frac{\mu_{eff}}{\mu_{bf}} = 1.475 - 0.319\emptyset + 0.051\emptyset^2 + 0.009\emptyset^3 \qquad (for\ 29\ nm\ CuO/water) \qquad (2.26)$$

Maiga *et al.* [11] performed a least-square curve fitting to Masuda et al. [19] and Wang et al. [20]'s experimental data of Al_2O_3/water and Al_2O_3/ethylene glycol nanofluids and developed a new correlations which are given by

$$\frac{\mu_{eff}}{\mu_{bf}} = 1 + 7.3\emptyset + 123\emptyset^2 \qquad (for\ Al_2O_3/water) \qquad (2.27)$$

$$\frac{\mu_{eff}}{\mu_{bf}} = 1 - 0.19\emptyset + 306\emptyset^2 \qquad (for\ Al_2O_3/ethyleneglycol) \qquad (2.28)$$

Pak and Cho [21] measured the viscosity of Al_2O_3 and TiO_2 particles dispersed in some base fluid and developed a correlation that are valid up to 10% volume concentration. The correlation is expressed as

$$\frac{\mu_{eff}}{\mu_{bf}} = 1 + 39.11\emptyset + 533.9\emptyset^2 \qquad (2.29)$$

Some researchers considered the temperature effect on viscosity of nanofluids by using temperature dependent viscosity model of the base fluid. The temperature dependent viscosity of the most used base fluid, water, can be found by the following

correlation

$$\mu_{water} = A \times 10^{B/(T-C)} \tag{2.30}$$

where A =2.41×10^{-5}, B =247.8 and C =140.

Although many researchers neglect the effect of temperature on nanofluid viscosity, there are also some researchers who use temperature effect in their viscosity correlations.

Abu-Nada [22] made two dimensional regression analyses and found the temperature and volume concentration dependent viscosity correlation by considering the experimental data of Nguyen et al. [18] for Al_2O_3 nanofluids. Their correlation is expressed as

$$\begin{aligned}\mu_{eff} = &- 0.155 - \frac{19.582}{T} + 0.794\emptyset + \frac{2094.47}{T^2} - 0.192\emptyset^2 - 8.11\frac{\emptyset}{T} - \frac{27463.863}{T^3} \\ &+ 0.0127\emptyset^3 + 1.6044\frac{\emptyset^2}{T} + 2.175\frac{\emptyset}{T^2}\end{aligned} \tag{2.31}$$

Duangthongsuk and Wongwises [23] conducted an experiment to find the viscosity of TiO_2/water nanofluid and developed a correlation that are valid between 0.2% and 2% volume concentration. Their correlation is described as

$$\frac{\mu_{eff}}{\mu_{bf}} = \mathrm{a} + \mathrm{b}\emptyset + \mathrm{c}\emptyset^2 \tag{2.32}$$

where

$$T = 15℃ \rightarrow a = 1.0226,\ b = 0.0477,\ c = -0.0112$$
$$T = 25℃ \rightarrow a = 1.013,\ b = 0.092,\ c = -0.015$$
$$T = 35℃ \rightarrow a = 1.0186,\ b = 0.112,\ c = -0.0177$$

Masoumi *et al.* [24] proposed a new correlation that considers the effect of the Brownian motion and particle size by using various experimental data of 13 and 28 nm Al_2O_3 nanoparticles in water. Their correlation is defined as

$$\mu_{eff} = \mu_{bf} + \frac{\rho_p V_B d_p^2}{72 C \delta} \tag{2.33}$$

where

$$\delta = \sqrt[3]{\frac{\pi}{6\emptyset} d_p} \tag{2.34}$$

and

$$v_B = \frac{1}{d_p} \sqrt{\frac{18 K_B T}{\pi \rho_p d_p}} \tag{2.35}$$

and

$$C = \mu_{bf}^{-1} [(-0.000001133 d_p - 0.000002771)\,\emptyset + (0.00000009 d_p - 0.000000393)\,] \tag{2.36}$$

Corcione *et al.* [14] investigated many experimental studies about viscosity of nanofluids and they developed a correlation which is described by

$$\frac{\mu_{eff}}{\mu_{bf}} = \frac{1}{1 - 34.87 (d_p / d_{bf})^{-0.3} \emptyset^{1.03}} \tag{2.37}$$

2.2. Studies About Forced Convective Heat Transfer of Nanofluids

In recent period, researchers have focused on the remarkable increase in the thermal conductivity due to the addition of nanoparticles in a solvent, and the related heat transfer efficiency leading to the decrease of energy consumption and equipment's size in a thermal system. Therefore, a lot of numerical or experimental works have been

published. In this chapter, some of these studies are shown.

2.2.1. Experimental Studies

Researchers have done many experiments to understand the reason of the significant heat transfer improvements of nanofluids.

Pak and Cho [21] studied turbulent friction and heat transfer properties of metal oxide particles dispersed in water in a pipe experimentally. They used Al_2O_3 with 13 nm particle size and TiO_2 with 27 nm. In their experiments, Reynolds number (Re_{nf}), Prandtl number (Pr_{nf}) and volume concentration ($\emptyset$) varied between 10^4-10^5, 6.5-12.3 and 0-3%, respectively. They found that the Nusselt number increases with increasing Reynolds number and volume concentration for fully developed turbulent flow. They developed a new Nusselt number (Nu_{nf}) correlation which is given by

$$Nu_{nf} = 0.021 Re_{nf}^{0.8} Pr_{nf}^{0.5} \tag{2.38}$$

for nanometer sized metal oxide particles dispersed in water under turbulent flow condition.

Xuan and Li [25] investigated turbulent heat transfer and flow characteristics of Cu/water nanofluid in a tube experimentally. In their experiments Reynolds number and volume concentration varied between 10000-25000 and 0-2%, respectively. For turbulent nanofluid flow inside a tube, they developed a new correlation which is given by

$$Nu_{nf} = 0.0059(1.0 + 7.6286\emptyset^{0.6886} Pe_d^{0.001}) Re_{nf}^{0.9238} Pr_{nf}^{0.4} \tag{2.39}$$

where the particle Peclet number can be expressed as

$$Pe_p = \frac{v d_p}{\propto_{nf}} \tag{2.40}$$

where v is the velocity, d_p is the particle diameter and $\propto_{nf}$ is the thermal diffusivity of nanofluid.

Williams *et al.* [12] studied the turbulent heat transfer characteristics of 46 nm size Al_2O_3/water and 60 nm size ZrO_2/water nanofluids experimentally. In their experiments Reynolds number, volume concentration and temperature varied between 9000-63000, 0.9-3.6% and 21-76℃, respectively. They compared their experimental data with the classical Dittus and Boelter [26] equation. They observed that their findings are in agreement with Dittus and Boelter equation. A similar experiment has also been conducted for laminar flow conditions. Rea et al. [27] investigated the heat transfer of 50 nm size Al_2O_3/water and 50 nm size ZrO_2/water nanofluids under laminar flow condition experimentally. The volume concentrations were 0.65%, 1.32%, 2.76% and 6%. They measured thermal conductivity and viscosity of Al_2O_3/water and ZrO_2/water nanofluid and developed property models. They showed that the heat transfer coefficients in the fully developed region are increased by 27%.

Duangthongsuk and Wongwises [28] investigated experimentally the heat transfer and pressure drop of 21 nm size TiO_2/water nanofluid under turbulent flow condition in a double tube counter-flow heat exchanger. In their experiments Reynolds number and volume concentration varied between 4000-16000 and 0.2-2%, respectively. They observed that the heat transfer coefficient of base liquid is smaller than the TiO_2/water nanofluid and also, the heat transfer coefficient of nanofluid increased with increasing Reynolds number and particle concentration. Also, they stated that the pressure drop value is increased by adding nanoparticles and this increase becomes more pronounced with increasing volume concentration. They proposed new correlations for the Nusselt number (Nu_{nf}) and friction coefficient (f_{nf}) of the nanofluid which are given by

$$Nu_{nf} = 0.074 Re_{nf}^{0.707} Pr_{nf}^{0.385} \emptyset^{0.074} \tag{2.41}$$

$$f_{nf} = 0.961 \emptyset^{0.052} {Re_{nf}}^{-0.375} \tag{2.42}$$

Fotukian and Esfahany [29] conducted experiments on turbulent convective heat transfer and pressure drop for 20 nm size Al_2O_3/water nanofluid flow inside a circular tube. In their experiments, Reynolds number and volume concentration varied between 5000-33000 and 0-0.2%, respectively. They stated that even adding small amount of nanoparticles increased heat transfer coefficient significantly. Also, the pressure drop for the nanofluid was found to be greater than that for the base fluid. In an another article [30], they investigated experimentally convective heat transfer and pressure drop characteristics of CuO/water nanofluid with less than 0.24% volume concentration inside circular tube under turbulent flow condition. They observed 20% pressure drop increase for 25% heat transfer coefficient enhancement. They argued that heat transfer enhancement ratio was not affected by the variation of volume concentration. Moreover, flow resistance increased even for very low concentrations of nanoparticle.

Sahin *et al.* [31] investigated experimentally convective heat transfer and pressure drop characteristics of Al_2O_3/water nanofluid under turbulent flow condition through circular tube. In their experiments, Reynolds number and volume concentration varied between 4000-20000 and 0-4%, respectively. They found that adding nanoparticles improved heat transfer rate until the volume concentration were up to 2% and also, the Nusselt number increased with increasing Reynolds number up to 1% volume concentration. They stated that viscosity and friction factor increases were much more dominant than the heat transfer enhancement when the volume concentration exceeds 1%.

Amrollahi *et al.* [32] researched the convective heat transfer coefficient of F-MWNT/ water nanofluid in entrance region of heated horizontal tube under both laminar and turbulent flow condition experimentally. They compared the heat transfer coefficient with respect to different parameters such as Reynolds number, mass fraction and bulk temperature in entrance region. They stated that nanoparticles and bulk temperature increased the heat transfer coefficient, but enhancement is much more in low bulk temperature at turbulent condition. Also, they claimed that increasing nanoparticle concentration has little effect on heat transfer enhancement under turbulent flow condition.

Chavan and Pise [33] studied convective heat transfer and flow characteristic of 30 nm size Al_2O_3 nanoparticle with a volume fraction between 0.1 to 1.0 and water nanofluid inside a pipe of 10 mm diameter and 1 m length. The Reynolds number of flow was changing between 8000 and 14000. They claimed that heat transfer improved with both Reynolds number and volume fraction. The heat transfer coefficient improved 36% for 8550 Reynolds number and 1% volume fraction when compared with base fluid. Also, they stated that the pressure drop significantly increase even the small addition of nanoparticles. Finally, they compared their experimental results with correlations which were already in literature.

Heyhat *et al.* [34] investigated the convective heat transfer and friction factor of 40 nm size Al_2O_3 nanoparticle with a volume concentration between 0.1 and 2% dispersed in water inside a circular tube with constant wall temperature and turbulent flow condition experimentally. They claimed that the heat transfer coefficient of nanofluid significantly higher than that of the base fluid. Also, heat transfer coefficient increased with increasing volume concentration. They stated that in a fixed volume concentration heat transfer enhancement was not influenced by changing Reynolds number. They compared their experimental results with traditional heat transfer coefficient and friction factor correlations.

Kayhani *et al.* [35] did some experiment about convective heat transfer and pressure drop properties of 15 nm size TiO_2/water nanofluid with 0.1, 0.5, 1.0, 1.5 and 2% volume concentration inside a uniformly heated horizontal circular tube under turbulent flow condition. They claimed that the heat transfer coefficient increased by increasing volume concentration and also it was not influenced from varying Reynolds number. They emphasized that the 8% improvement of Nusselt number was observed with 2.0% volume concentration at 11800 Reynolds number.

Wusiman *et al.* [36] researched the forced heat transfer characteristic of Cu/wa-ter nanofluid with different volume concentration under varying Reynolds number condition experimentally. They found that the convective heat transfer coefficient increased with volume concentration in both laminar and turbulent flow. However, enhancement

of heat transfer coefficient was much more in laminar flow regime. Also, the heat transfer coefficient decreased sharply when flow became turbulent. In turbulent flow regime, the heat transfer coefficient increased slowly with increasing concentration or Reynolds number when compared with laminar flow regime.

Hojjat *et al.* [37] studied forced convection heat transfer of Al2O3, TiO2 and CuO with carboxymethyl cellulose (CMC) non-Newtonian (shear thinning) nanofluids inside circular pipe under constant wall temperature condition in turbulent flow regime experimentally. They observed that the convective heat transfer coefficients of nanofluids were bigger than that of the base fluid. They stated that enhancement of heat transfer coefficient increased with increasing the Peclet number and volume concentration. Also, they compared their experimental results with correlations which are already presented in literature for purely viscous non-Newtonian fluids. In addition, they developed a new correlation which involves Reynolds and Prandtl numbers.

Azmi *et al.* [38] investigated the heat transfer coefficient and friction factor of SiO_2/water nanofluid with up to 4% volume concentration inside circular tube at a 30°C bulk temperature with Reynolds number range of 5000-27000 under constant heat flux condition experimentally. They found that Nusselt number and friction factor were greater than that of base fluid. Also, they stated that the pressure drop increased with volume concentration up to 3.0% and decreased after that value. In addition, the friction factor decreased with increasing Reynolds number at any concentration.

Merilainen *et al.* [39] studied convective heat transfer of water based Al_2O_3, SiO_2 and MgO nanofluids with up to 4% volume concentration inside circular tube under constant wall temperature condition experimentally. They found that average convective heat transfer coefficients of all nanofluids are bigger than that of base fluid. This enhancements were up to 40% when Reynolds number kept constant around 3000-10000. However, the significant pressure losses are occurred because the dynamic viscosities are increased. Because of that, they defined the convective heat transfer efficiency for comparing the heat transfer enhancement with pressure loss enhancement. They claimed that when the enhancement of volume concentration exceeds 2%,

the heat transfer rate increases but also heat transfer efficiency decreases because of increasing pressure losses.

Anoop *et al.* [40] researched heat transfer of 45 and 150 nm size Al_2O_3/water nanofluids under laminar flow condition experimentally. They stated that the heat transfer increase is higher for smaller size nanoparticles.

Wen and Ding [41] investigated forced convective heat transfer of Al_2O_3/water nanofluid inside a copper tube under laminar flow condition experimentally. They observed that the heat transfer increase is more pronounced in entrance region (developing flow) and they stated that this situation can not be explained only by the enhancement of the thermal conductivity enhancement. They said that the non-uniform distribution of viscosity and thermal conductivity due to the particle migration triggered this phenomenon.

Yang *et al.* [42] studied experimentally the convective heat transfer of non-spherical graphite water nanofluid under laminar flow regime in a horizontal tube. They observed that the temperature, the Reynolds number and the volume concentration are very important for heat transfer of the nanofluid and the heat transfer coefficient increased with increasing the Reynolds number and the volume concentration.

Heris Zeinali *et al.* [43] investigated experimentally the heat transfer enhacement of Al_2O_3/water and CuO/water nanofluids under laminar flow condition with constant wall temperature. They observed that the heat transfer increase with increasing volume concentration and Peclet number for both nanofluids. Moreover, they found that the heat transfer increase of the Al_2O_3/water nanofluid is higher than that of the CuO/water nanofluid, however, there is no significant difference between both nanofluid types in terms of heat transfer enhancement at a low concentration.

Sultan [44] experimentally examined the effect of 25 nm size Al, 30 nm size Al_2O_3 and 50 nm size CuO nanoparticles dispersed in water on heat transfer under

fully developed laminar flow condition inside horizontal and inclined pipe with uniform heat flux and volume concentration range between 0.25 and 2.5%. The enhancement of the Nusselt number is found to be 45%, 31% and 25% for Al, Al_2O_3 and CuO water nanofluids, respectively.

Sajadi and Kazemi [45] investigated experimentally the heat transfer and pressure drop characteristics of TiO_2/water nanofluid which have 0.05% and 0.25% volume concentration under turbulent flow regime. They observed that even small amount of nanoparticles increased the heat transfer coefficient of the base fluid and the increase in the pressure drop is not significant compared to the heat transfer enhancement.

Sundar *et al.* [46] examined the heat transfer coefficient and the friction factor characteristics of 36 nm Fe_3O_4/water nanofluid in a circular tube under turbulent flow condition with volume concentration range between 0 and 0.6%. They stated that the heat transfer coefficient and the friction factor increase with increasing volume concentration that 30.96% enhancement in heat transfer and 10% friction factor are found for 0.6% volume concentration.

Wang *et al.* [20] researched pressure drop and heat transfer characteristics of carbon nanotubes nanofluids under laminar flow condition inside a circular pipe. They claimed that the friction factor can be found by using Hagen-Poiseuille theory. The 70% and 190% enhancement in heat transfer are found at a Reynolds number of 120 for 0.05% and 0.24%, respectively. Moreover, they stated that the required pumping power can be neglected since it is very low for low volume concentrations.

Nasiri *et al.* [47] investigated experimentally the heat transfer enhancement of Al2O3/water and TiO_2/water nanofluids under turbulent flow condition with constant wall temperature. They researched the effect of the Reynolds number and the volume concentration. They found that the enhancement of the heat transfer increases with increasing volume concentration and Reynolds number.

Ding *et al.* [48] experimentally examined forced convective heat transfer behavior of water and ethylene glycol based TiO_2, titanate nanotubes and carbon nanotubes nanofluids. They observed that the enhancement of heat transfer is higher than the enhancement of the thermal conductivity and they stated that the effect of the particle migration on thermal boundary layer thickness is the reason of this result. Moreover, a decrease in heat transfer was observed at low Reynolds number for ethylene glycol based TiO_2 nanofluid.

Hwang *et al.* [49] researched the convective heat transfer and pressure drop behavior of Al_2O_3/water nanofluid under laminar flow condition inside a uniformly heated pipe. They stated that the friction factor of the nanofluid can be found by using classical Darcy's equation. The convective heat transfer coefficient increased 8% for 0.3% volume concentration.

The similar results can not be obtained even though many experiments have been studied about the heat transfer of nanofluids. This may be due to differences in experimental test conditions. Therefore, experiments should be supported numerically as well. It can be understand that the forced convective heat transfer of nanofluids is affected by many parameters. However, the reason behind the increase in heat transfer can not be explained not only by the thermal conductivity enhancement, but also the effect of the particle migration on the thermal boundary layer. Due to the importance of forced convective heat transfer and pressure drop behavior, both experimental and numerical works should be investigated and the reliable numerical models and correlations should be developed.

2.2.2. Numerical Studies

Many researchers have also investigated numerically thermal and hydrodynamic properties of nanofluids and using mainly single phase models with enhanced fluid properties. However, there are some studies showing that two phase models such as mixture, Eulerian and the discrete phase model (Eulerian Lagrangian approach) give better agreement with experimental correlations.

2.2.2.1. The single phase model. The single phase flow model with enhanced nanofluid properties is one of the most used flow model due to its simplicity and it gives reasonable results for many situations.

Maiga *et al.* [11] studied numerically the turbulent flow and heat transfer characteristics of Al_2O_3/water nanofluid inside a pipe with constant heat flux boundary condition, using the single phase model. They developed a Nusselt number correlation given by

$$Nu_{nf} = 0.085 Re_{nf}^{0.71} Pr_{nf}^{0.35} \tag{2.43}$$

which is valid for $10^4 < Re_{nf} <$ 5 x 10^5, 6.6 $< Pr_{nf} <$ 13.9 and $0 < \emptyset < 10\%$.

Namburu *et al.* [50] investigated numerically the flow and heat transfer properties of ethylene glycol and water mixture based CuO, Al_2O_3 and SiO_2 nanofluids inside a circular tube with constant wall heat flux condition for turbulent flow, using the single phase model. In their simulations, Reynolds number and volume concentration varied between 10000-100000 and 0-6%, respectively. They considered that all fluid properties depend on temperature and found that Gnielinski [51] correlation for Nusselt number is in good agreement with their numerical results. They observed that nanofluids which have smaller diameter nanoparticles have greater viscosity and Nusselt number. They stated that CuO nanofluid with 6% volume concentration shows 35% heat transfer enhancement in terms of the Nusselt number.

Bayat and Nikseresht [52] studied the thermal performance and pressure drop properties of Al_2O_3/EG-water mixture in circular horizontal tube under turbulent flow condition using the single phase model. In their simulations, Reynolds number and volume concentration varied between 10000-100000 and 1-10%, respectively. They argued that the k- turbulence model with near wall treatment gives better predictions compared to other turbulence models. They found that for a fixed Reynolds number, the convective heat transfer coefficient increases with increasing particle concentration. Moreover, at the same Reynolds number adding nanoparticles to base fluid increases

the pressure drop and required pumping power. They concluded that using nanofluids in turbulent flow condition is not practical due to the increase in the pumping power.

Kumar [53] investigated heat transfer of Al_2O_3 nanofluid inside pipe under constant wall temperature numerically by using single phase approach. They stated that the heat transfer enhancement is not as important as in the turbulent regime. They claimed that single phase approach is not valid for turbulent flow condition.

Hatami and Okhovati [54] analyzed the friction coefficient, pressure drop and viscous drag of water and ethylene glycol based oxide nanofluids under turbulent flow condition inside a pipe numerically by using Fluent software. They found that friction factor, pressure drop and viscous drag increase when the volume fraction increases. However, this enhancement is not significant when the volume fraction is low. Also, as Reynolds number increases also the pipe wall viscous drag force and the drag force increase, but the friction factor decreases. In addition, they claimed that using nanofluids has little effect on developed velocity field.

Shedid [55] studied thermal characteristic of water based Al_2O_3 and TiO_2 nanofluids for turbulent annular flow under constant wall temperature condition numerically by using Spalart-Allmaras turbulence modelling. They validated their model with Gnielinski correlation [51] for pure water. They tried to understand the effect of different concentration ratios and Peclet numbers. They claimed that Spalart-Allmaras turbulence model predict more accurate than k- model. Also, they found that the Nusselt number increases with increasing Peclet number and concentration ratio.

Moraveji and Beheshti [56] investigated forced convection heat transfer of carboxymethylcellulose aqueous based 10, 25, 40 nm size Al_2O_3, TiO_2 and CuO, respectively, non-Newtonian nanofluids under constant wall temperature with turbulent flow condition inside horizontal tube numerically by using CFD softwares. They researched effects of nanoparticle type and Peclet number on the convective heat transfer coefficient. They proposed a new correlation for Nusselt number by using their CFD results. Then, they compared their correlation with experimental data in literature.

Kumar and Ganesan [57] studied the heat transfer increment of aluminum oxide nanofluid which has low and high volume fractions in turbulent pipe flow under constant wall temperature condition numerically by using single phase approach. They found that using up to 1% volume fraction of nanofluid enhances the heat transfer coefficient. The Nusselt number and the friction factor results of simulations are good agreement with experimental data in literature for the low volume fractions which are up to 0.5%. However, for high volume fractions which are between 1% and 6%, there are a significant error between experimental data and numerical results when single phase approach is used.

Aghaei *et al.* [58] investigated the flow and heat transfer characteristics of 25, 33, 75, and 100 nm size Al_2O_3/water nanofluid with 0, 0.001, 0.1, 0.2, and 0.4 volume fractions inside a tube with constant 310 K wall temperature under turbulent flow condition which have 10000, 20000, 30000, and 100000 Reynolds number numerically. They used the finite volume method and SIMPLE algorithm for simulations. They found that average Nusselt number increases with increasing Reynolds number. And also, there is a non-uniform relation between average Nusselt number and volume fractions. They claimed that the enhancement of Reynolds number causes reduction of skin friction factor for all volume fraction values.

Hussein *et al.* [59] did simulation about the friction factor and Nusselt number of 27 nm size TiO_2/water nanofluid with 0.25%, 0.5%, 0.75% and 1% volume fractions inside a horizontal straight tube with constant heat flux 5000 W/m2 under turbulent flow condition which have Reynolds number from 10000 to 100000. They found that increasing volume fraction cause improvement in Nusselt number and friction factor. Also, their results are in good agreement with experimental data in literature.

Ozerinc *et al.* [60] investigated numerically the heat transfer enhancement of nanofluids with volume concentration range between 1% and 2.5% under fully developed laminar flow condition. They compared their numerical results with Heris Zeinali et al.'s [43] experimental results. They stated that the single phase model gives accurate results compared to experimental results. Moreover, the model's accuracy can be

improved by using variable thermal conductivity model and variable thermal dispersion model.

Azimi and Kalbasi [61] examined numerically the forced convective heat transfer of nanofluid in the entrance region of the pipe under laminar flow condition. They stated that the dynamic part that includes the Brownian motion of nanofluid' s thermal conductivity has less influence on heat transfer coefficient when compared to the static part which considers nanolayer around nanoparticle.

2.2.2.2. The two phase models. There are some articles that consider two phase models with the single phase model.

Behzadmehr *et al.* [62] numerically researched the heat transfer behavior of Cu/ water nanofluid in a circular tube under turbulent flow condition with constant wall heat flux. They compared their numerical results with Xuan and Li [25]'s experimental results and they observed that the single phase model can not predict the Nusselt number in some cases.

Bianco *et al.* [63] studied numerically the turbulent forced convection flow of 38 nm size Al_2O_3/water nanofluid inside a circular tube with uniform wall heat flux condition, using the single phase and two phase mixture models. In their simulations, Reynolds number and volume concentration varied between 10000-100000 and 0-6%, respectively. They found that increasing Reynolds number and volume concentration lead to further enhancement of the heat transfer rate. They stated that the mixture model is reliable although the accuracy of the model may be improved using better thermophysical property relations. They also observed that the single phase model gives closer results to Maiga *et al.* [11]'s correlation and the mixture model gives closer results to Pak and Cho [21]'s correlation.

Behroyan *et al.* [64] compared five different models which are Newtonian and Non-Newtonian single phase models, Eulerian-Eulerian, mixture and Eulerian Lagrangian

two phase models, using finite volume method to investigate the convective heat transfer of Cu/water nanofluid in a tube with constant wall heat flux, under turbulent flow condition. In their simulations, Reynolds number and volume concentration varied between 10000-25000 and 0-2%, respectively. They observed that the non-Newtonian single phase model results are not in good agreement with literature data for the Nusselt number prediction, and the Eulerian-Eulerian model gives results with higher error except for 0.5% volume concentration. Finally, they recommended the Newtonian single phase and Eulerian-Lagrangian two phase models for accurate prediction.

Hejazian and Moraveji [65] studied forced convection of 30 nm size dilute TiO_2/ water nanofluid inside a horizontal circular tube under turbulent flow condition numerically. They used 2 different approaches for numerical analysis which are single phase and mixture model. They stated that the convective heat transfer coefficient increases when Reynolds number and volume concentration increase. Also, they claimed that the mixture model is more accurate when compares with experimental data than the single phase approach.

Low *et al.* [66] investigated the heat transfer enhancement of different nanoparticles under turbulent flow condition inside circular tube numerically. They used single phase, mixture and Eulerian models with 3D flow simulation. They studied effect of drag and lift forces for different volume concentration and Reynolds number. They found that heat transfer coefficient of nanofluids is better than that of base liquid and also the heat transfer coefficient increases with increasing Reynolds number and volume concentration. They claimed that their simulation results are in good agreement with experimental results in literature. They said that the mixture model predicts more correctly when compared to Eulerian model.

Esfandiary *et al.* [67] analyzed forced convection heat transfer of Al_2O_3/water nanofluid inside a pipe with constant wall heat flux under turbulent flow condition which have Reynolds number between 3000 and 9000 numerically by using single and two phase models. They considered that the thermal and flow properties of nanofluid are depend on temperature and volume fraction. They found that increasing Reynolds

number and volume fraction cause further enhancement of heat transfer coefficient. In addition, the skin friction coefficient is not influenced from increasing volume fraction, but the skin friction coefficient decreases with increasing Reynolds number. They claimed that their numerical results are in good agreement with experimental results when the single phase model is used.

Minea [68] studied forced convection heat transfer of Al_2O_3/water nanofluid inside horizontal tubes under turbulent flow condition numerically. They considered 5 different models to find the thermal and flow properties of nanofluid. The 2.33-26.45% enhancement of heat transfer coefficient is observed for a constant Reynolds number when compared with that of water.

Göktepe *et al.* [69] numerically investigated the flow and heat transfer characteristics of nanofluid at the entrance region of pipe with constant wall heat flux. They compared the single phase model with and without thermal dispersion effect, Eulerian and mixture two phase model with experimental results from the literature. They observed that two phase models give better results in terms of heat transfer coefficient and friction factor at the entrance region.

Fard *et al.* [70] researched the convective heat transfer behavior of Cu, CuO and Al_2O_3 dispersed in water nanofluids inside a pipe under laminar flow condition with constant wall temperature numerically. They used both single phase and two phase models. They stated that the two phase model gives more precise results when compared to the single phase model according to Heris Zeinali et al. [43]' s experimental results.

Kalteh *et al.* [71] studied the forced convective heat transfer of Cu/water nanofluid inside microchannel with constant heat flux under laminar flow condition numerically by using Eulerian model. They stated that velocity and temperature differences between the nanoparticle and the base fluid phases are negligible. Moreover, the heat transfer enhancement result of two phase model is higher than that of single phase model.

Moraveji and Esmaeili [72] investigated forced convection heat transfer of fully developed laminar Al_2O_3/water nanofluid flow inside a heated pipe by using both single and two phase models. They developed a Nusselt number correlation and stated that the correlation is in very good agreement with Dittus-Boelter equation. They stated that the results of single phase and two phase models are not very different from each other since the maximum difference is 11%.

Kondaraju and Lee [73] examined the heat transfer behavior of 100 nm size Cu and 80 nm size Al_2O_3 dispersed in water nanofluid by using Eulerian-Lagrangian model to investigate the mechanism of heat transfer enhancement. They reported that the results of their model are in a good agreement with Xuan and Li [25] and Murshed et al. [74]'s experimental results.

Davarnejad and Jamshidzadeh [75] investigated the flow and heat transfer characteristics of MgO/water nanofluid under turbulent flow condition inside a circular tube numerically by using single phase, volume of fluid (VOF) and mixture models. They stated that two phase models predict better than the single phase model especially at high volume concentrations.

Lotfi *et al.* [76] numerically studied the laminar forced convection characteristics of Al_2O_3/water nanofluid which has volume concetration range of 2% to 7% inside a horizontal tube with constant heat flux. They stated that the heat transfer enhancement prediction of the two phase mixture model is more accurate than the single phase and the two phase Eulerian model.

2.3. Research Gaps

From the literature review, it can be understand that the precise predictions can not be obtained by the proposed numerical simulations. Researchers tried to improve precision with using different flow models. It can be seen that each flow model is good at prediction of different nanofluid behavior. One can investigate the Brownian motion and thermal dispersion effect by using the single phase model. Furthermore, the effect

of slip velocity between nanoparticle and base fluid phases can be examined with the mixture model. The Eulerian model can investigate the drag force and interphase heat transfer. Although some researchers claimed that the two phase model is better, some investigators suggested the single phase model. Therefore, it is still not possible to determine which model is more suitable in which situations. There is a need for a numerical analysis method that is valid for wide range of Reynolds number and volume concentration.

For the single phase model, although various effective thermophysical property models have been tried to evaluate effective properties, it is not mentioned that why those models were selected and the chosen models have not been compared with other models to determine the mechanism of heat transfer enhancement in many articles. In two phase modelling, the determination of the properties of the solid phase is hardly mentioned since there is no direct correlation for the solid phase. Generally, the properties of the solid phase are found by adapting to effective thermophysical models used in the single phase modelling. The fact that the reliability of the thermophysical models is not so good decrease the success of this method. Moreover, it is aimed to remove the dependence on thermophysical property models for two phase modelling in this study. To do that, the granular model is used to define the solid phase and the actual thermal conductivity value of the solid nanoparticle is applied in numerical simulations. The viscosity of the solid phase is defined according to Miller and Gidaspow [77] equation which is originally developed for dense gas-solid flow.

Although there are many studies comparing the single and two phase models, most of these studies are for laminar flow. There are few studies in this sense for the turbulent flow regime, especially for low concentrations. In most of these studies, the laminar and turbulent flow were not compared each other with using two phase models. Moreover, some studies using the single phase model do not consider the effect of the temperature and the Brownian motion. Also, there is a lack in the literature in terms of studies comparing the heat transfer enhancement and its mechanisms between laminar and turbulent flow of nanofluids.

Generally, the heat transfer behavior of nanofluids is studied, the pressure drop effect is not considered. Therefore, the optimum working condition should be determined according to the flow and heat transfer characteristics of the chosen nanofluid. Moreover, most of the numerical studies have been tried to be proved based on a single experimental data. Therefore, the validity of these studies is questionable.

3. MODELLING OF THE FORCED CONVECTION OF NANOFLUIDS

3.1. Introduction

In this chapter, the turbulent forced convection of Al_2O_3/water nanofluid is investigated inside a circular tube by using different numerical flow models.

Simulations are carried out for four different experimental data, using the single phase and the two phase mixture and Eulerian models. For turbulent flow of dilute ($\emptyset < 0.5\%$) Al_2O_3/water and CuO/water nanofluid simulations, Fotukian and Esfahany [29, 30]' s experimental results (Experiment 1 and 4) are used for validation. In the Experiment 1, the parameter ranges are: $12000 < Re < 32000$, $15℃ < T_b < 70℃$ and $0.03\% \leq \emptyset \leq 0.135\%$. In the Experiment 4, the parameter ranges are: $10000 < Re < 32000$, $20℃ < T_b < 75℃$ and $0.015\% \leq \emptyset \leq 0.236\%$. For turbulent flow of Al_2O_3/water nanofluid with 1.8% and 3.6% volume concentration, Williams *et al.* [12]' s experimental results (Experiment 2) are used. In the Experiment 2 the parameter ranges are: $8000 < Re < 31000$, $21℃ < T_b < 80℃$. Finally, to compare the flow and heat transfer characteristics under laminar and turbulent flow conditions, Rea *et al.* [27]' s experimental results (Experiment 3) for laminar flow of Al_2O_3/water nanofluid with 1.32% and 2.76% volume concentrations are also used. In the Experiment 3 the parameter ranges are: $500 < Re < 2000$, $20℃ < T_b < 40℃$.

The average and local heat transfer coefficients, the Nusselt number, the friction factor and the pressure drop results will be displayed and compared. This study can be used when understanding some effect on heat transfer and pressure drop of nanofluids and selecting suitable thermophysical property and flow models.

3.2. Basic Definitions About Flow and Heat Transfer

3.2.1. Flow Analysis

The Reynolds number is a important parameter to determine whether the flow is laminar or turbulent. For the flow in a circular tube, the Reynolds number is defined as

$$Re = \frac{\rho v D}{\mu} \tag{3.1}$$

where ρ is the density of the fluid, D is the diameter of the pipe, V is the velocity and μ is the viscosity. The flow in a circular pipe is considered laminar for Re<2300 and turbulent for Re>4000. The entrance length is defined as the distance traveled in the pipe before the flow is fully developed. The fully developed flow can be defined as the section in which the pressure gradient and shear forces are balanced each other and the velocity profile remains unchanged. In all simulations of this study, the pipe length (L) to pipe diameter (D) ratio is above 10, such that the entrance region is very small and it can be assumed that the flow is fully developed almost in the entire region of the pipe.

The fluid velocity on a tube wall is zero because of the no-slip condition and is maximum at the center of the pipe because of the minimum shear force. Because the velocity value changes along the y direction of the pipe, the mean or average velocity is defined. This value remains constant along the pipe cross section when the flow is considered as an incompressible.

The pressure drop is very important since the pump used in the heat transfer system is directly related to the power requirement. Pressure drop can be defined as

$$\Delta P = f \rho \frac{L}{D} \frac{v^2}{2} \tag{3.2}$$

and pumping power can be written as

$$W_{Pump} = \Delta P.Q \tag{3.3}$$

where ΔP is the pressure drop, f is the friction factor, L is the length of the pipe and Q is the volumetric flow rate.

The friction factor, f, is the dimensionless parameter that depends on the Reynolds number and wall roughness. Since the pipe is considered as a smooth pipe in this study wall roughness is neglected. For a laminar fully developed flow, the friction factor is defined by

$$f = \frac{64}{Re} \tag{3.4}$$

For fully developed turbulent flow, there are different friction factor correlations in literature. The most common ones, Blasius [78] for $Re \leq 30000$ and McAdams [79] for $Re > 30000$ are listed below,

$$f = 0.316Re^{-0.25} \qquad for\ Re \leq 30000 \tag{3.5}$$

$$f = 0.184Re^{-0.2} \qquad for\ Re > 30000 \tag{3.6}$$

Moreover, Petukhov [80] developed a correlation for turbulent friction factor which is described by

$$f = (0.79\ln(Re)\ - 1.64)^{-2} \tag{3.7}$$

The wall shear stress is defined by

$$\tau = \frac{f\rho v^2}{8} \tag{3.8}$$

and can be calculated by using one of the friction factor correlations described above.

3.2.2. Thermal Analysis

The energy change between the pipe inlet and outlet of the flowing fluid inside a pipe can be explained by the conservation of energy principle. According to that, the heat transferred from the pipe surface to the fluid is equal to the energy change. The energy change of the fluid is described as

$$Q = \dot{m}c_p(T_o - T_i) \tag{3.9}$$

where $\dot{m}$ is the mass flow rate of the fluid, c_p is the specific heat of the fluid, T_o is the outlet temperature and T_i is the inlet temperature. The amount of heat transferred from the pipe surface by convection is described by Newton's law of cooling

$$Q = hA_{pipe}(T_w - T_b) \tag{3.10}$$

where h is the convective heat transfer coefficient of the fluid, T_w is the pipe wall temperature and T_b is the bulk temperature of the fluid and described as

$$T_b = \frac{\int_A \rho v c_p T dA}{\int_A \rho v c_p dA} \tag{3.11}$$

The heat transfer characteristic of a fluid can be determined according to the heat transfer coefficient. However, the heat transfer coefficient is a dimensional number and varies according to the flow geometry and wall heat flux or wall temperature values.

Therefore, dimensionless Nusselt number can be defined as,

$$Nu = \frac{hD}{k} \tag{3.12}$$

where k is the thermal conductivity of the fluid.

There are many correlations to describe Nusselt number in literature. Gnielinski [51] correlation for fully developed turbulent pipe flow is used in this study and it can be described as

$$Nu = \frac{\left(\frac{f}{8}\right)(Re - 1000)\,Pr}{1 + 12.7\left(\frac{f}{8}\right)^{0.5}(Pr^{\frac{2}{3}} - 1)} \tag{3.13}$$

where Pr is the Prandtl number of the fluid and can be defined as

$$Pr = \frac{c_p \mu}{k} \tag{3.14}$$

where μ is the viscosity of the fluid. The friction factor, f can be found from Petukhov correlation.

There is a relation between heat transfer and flow characteristics of a fluid in a flow field. The Reynolds analogy explains this relation by associating the flow and thermal parameters. If the properties of a given flow field can be defined, the knowledge of thermal behavior can also be obtained through the Reynolds analogy which can be explained as

$$\frac{f}{8} = St \tag{3.15}$$

where St is the Stanton number and can be defined as

$$St = \frac{Nu}{RePr} \tag{3.16}$$

However, the Reynolds analogy is valid only when the Prandtl number is unity. Chilton and Colburn [81] defined a improved version of Reynolds analogy which can be described as

$$\frac{f}{8} = StPr^{j} \tag{3.17}$$

to expand the range of Prandtl number. j is called Colburn factor and is taken as 2/3. Equation 3.17 is valid for $0.6 < Pr < 60$.

3.3. Methodology

3.3.1. Geometry and Boundary Conditions

The typical geometry of the flow domain is shown in Figure 3.1. The uniform axial fluid velocity at the inlet is denoted as vin, and the fluid inlet temperature, as Tin. At the exit, the outlet pressure is equal to the atmospheric pressure. In the two phase model, the inlet velocity is assumed the same for two phases. On the wall, no slip boundary conditions are imposed together with uniform wall heat flux (q). The tube diameter, tube length, inlet velocity, inlet temperature and the wall heat flux values are determined according to the four experimental articles mentioned before. In Experiment 1 and 4 (Domain 1), the tube diameter and tube length are 0.005 m, 1 m respectively, in Experiment 2 (Domain 2), the tube diameter and tube length are 0.0094 m, 2.819 m respectively, and in Experiment 3 (Domain 3), the tube diameter and tube length are 0.0045 m, 1.01 m respectively.

3.3.2. Thermophysical Properties of The Nanofluid

For the single phase model, the suspension formed by the base fluid and nanoparticles is treated as a single fluid with equivalent properties.

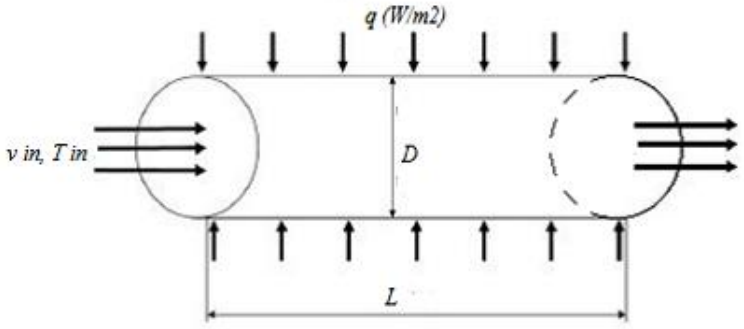

Figure 3.1. The geometry of the flow problem.

To evaluate the density and specific heat of the nanofluid, the following relations are used

$$\rho_{nf} = (1 - \emptyset)\,\rho_{bf} + \emptyset\rho_p \tag{3.18}$$

$$(\rho c_p)_{nf} = (1 - \emptyset)\,(\rho c_p)_{bf} + \emptyset(\rho c_p)_p \tag{3.19}$$

There are many different temperature dependent or independent relations which have been proposed in the literature, to define the thermal conductivity and the viscosity of the nanofluid, and the simulation results depend strongly on the choice of proper relations. Therefore, it is necessary to select a property model according to the temperature and concentration ranges and the nanofluid type, used in the applications.

For the viscosity, Model 1V used in this study, is proposed by Williams *et al.* [12] for Al_2O_3/water nanofluid and can be described as

$$\mu_{nf}\,(\emptyset, T) = \mu_{bf}\,(T)\ \exp[4.91\emptyset/(0.2092 - \emptyset)] \tag{3.20}$$

This model is obtained from experimental results of Williams *et al.* and is only valid for the temperature and volume concentration ranges used in their experiments. It is applicable for 1% <∅< 6% and 21℃<T< 80 ℃.

The second chosen viscosity model, Model 2V, is Einstein [15]'s model which is generally applicable for dilute nanofluids (∅< 0.5%) and can be written as

$$\frac{\mu_{nf}}{\mu_{bf}} = (1 + 2.5\emptyset) \tag{3.21}$$

For the thermal conductivity, Model 1 is the model proposed by Yu and Choi [4]. This model does not consider Brownian motion and temperature effect, and can be described as

$$\frac{k_{nf}}{k_{bf}} = \frac{k_p + 2k_{bf} + 2(k_p - k_{bf})(1+\beta)^3\emptyset}{k_p + 2k_{bf} - (k_p - k_{bf})(1+\beta)^3\emptyset} \tag{3.22}$$

where β=0.1, and the model is applicable for ∅> 1%.

Model 2 is the Williams *et al.* [12]'s model, derived from curve-fitting of their experimental results for Al_2O_3/water nanofluid. The Model 2 is described as

$$k_{nf}(\emptyset, T) = k_{bf}(T)\ (1 + 4.5503\emptyset) \tag{3.23}$$

This model is applicable for 1% <∅< 6% and 21℃<T< 80 ℃.

Model 3 is the Chon *et al.* [6]'s model which is temperature dependent and considers Brownian effects. The Model 3 is described as

$$\frac{k_{nf}}{k_{bf}} = 1 + 64.7\emptyset^{0.746}\left(\frac{d_{bf}}{d_p}\right)^{0.369}\left(\frac{k_p}{k_{bf}}\right)^{0.7476} Re_p^{1.2325} Pr^{0.9958} \tag{3.24}$$

where

$$Pr=\frac{c_{p,bf}\mu_{bf}}{k_{bf}} \tag{3.25}$$

and

$$Re_p=\frac{\rho_{bf}K_BT}{3\pi\mu_{bf}^2\gamma} \tag{3.26}$$

and K_B= 1.3806×10^{-23} J/K is the Boltzman constant and γ is the mean free path of water molecule taken as 0.17 nm. The model is applicable for 1% <$\emptyset$< 4% and 21°C <T< 71°C.

Model 4 is the Patel *et al.* [7]'s model which is temperature dependent and considers Brownian effects. The Model 4 is described as

$$\frac{k_{nf}}{k_{bf}}= 1+\frac{d_{bf}}{d_p}\frac{\emptyset}{1-\emptyset}\frac{k_p}{k_{bf}}(1+25000\ Pe_p) \tag{3.27}$$

where Pe_p is the particle Peclet number described as

$$Pe_p=\frac{2K_BT}{\pi\mu_{bf}d_p^2}\frac{d_p}{\propto_{bf}} \tag{3.28}$$

This model is applicable for 1% <$\emptyset$< 8% and 20°C <T< 50°C. It should be considered that Model 3 and Model 4 have different type of Brownian velocity definition.

It should be noted that the viscosity models (Model 1V and Model 2V) are used in the single phase formulation, however in the two phase mixture and Eulerian formulations, the granular model is chosen to estimate the solid phase viscosity.

All properties are evaluated at bulk temperature. The bulk temperature, T_b is described as

$$T_b = \frac{T_{b,in} + T_{b,out}}{2} \tag{3.29}$$

where the inlet and outlet bulk temperatures are extracted from experimental results.

3.3.3. Governing Equations

For turbulent flow formulation, the Reynolds-Averaged Navier-Stokes (RANS) approach is used where the flow variables are decomposed into their mean and fluctuating parts and the governing equations are statistically averaged in time. The nanofluid is assumed to be Newtonian and incompressible.

3.3.3.1. Single Phase Formulation. In the steady-in-the-mean single phase formulation, mass conservation equation can be expressed as

$$\nabla . \left(\rho_{nf} \overline{V} \right) = 0 \tag{3.30}$$

where $\overline{V}$ is the time averaged (mean) velocity vector and ρ_{nf} is the nanofluid density.

The momentum equation for the single phase model can be expressed as

$$\nabla . \left(\rho_{nf} \overline{VV} \right) = -\nabla \overline{p} + \nabla . (\mu_{nf} \nabla \overline{V} - \rho_{nf} \overline{V'V'}) \tag{3.31}$$

where $\overline{p}$ is the time averaged pressure, μ_{nf} is the nanofluid viscosity and V' represents the fluctuations in the velocity vector.

Also, the energy equation can be expressed as

$$\nabla . \left(\rho_{nf} c_{p,nf} \overline{VT} \right) = \nabla . (k_{nf} \nabla \overline{T} - \rho_{nf} c_{p,nf} \overline{V'T'}) \tag{3.32}$$

where k_{nf} is the nanofluid thermal conductivity, $c_{p,nf}$ is the nanofluid specific heat, $\overline{T}$ is the time averaged temperature and $T^{'}$ represents the fluctuations in the temperature.

The terms, $(\rho_{nf}\overline{V'V'})$ and $(\rho_{nf}c_{p,nf}\overline{V'T'})$, in the governing Equation 3.31 and 3.32, represent the turbulent stress and the turbulent heat flux, respectively.

3.3.3.2. Two Phase Formulation. For the two phase formulation, the first model we choose is the mixture model. The continuity equation of the mixture model can be expressed as

$$\nabla.\left(\rho_m\overline{V_m}\right)=0 \tag{3.33}$$

where ρ_m is the mixture density and expressed as

$$\rho_m=\sum_{k=1}^{n}\emptyset_k\rho_k \tag{3.34}$$

and $\emptyset$ is the volume concentration, the subscript k is the phase number, n is the number of phases, $\overline{V_m}$ is the time-averaged mixture velocity given by

$$\overline{V_m}=\frac{\sum_{k=1}^{n}\emptyset_k\rho_k\overline{V_k}}{\rho_m} \tag{3.35}$$

The momentum equation of the mixture model can be written by summing the momentum equations of each phase (liquid and solid) and described as

$$\nabla.\left(\rho_m\overline{V_m}\ \overline{V_m}\ \right)=-\nabla\overline{p}+\nabla.[\mu\nabla\overline{V_m}\ +\sum_{k=1}^{n}\emptyset_k\rho_k\overline{V_k^{'}V_k^{'}}]+\nabla.(\sum_{k=1}^{n}\emptyset_k\rho_k\overline{V_{dr,k}V_{dr,k}}) \tag{3.36}$$

where the mixture viscosity μ_m can be defined as

$$\mu_m=\sum_{k=1}^{n}\emptyset_k\mu_k \tag{3.37}$$

The secondary (solid) phase is treated as granular and an equivalent dynamic viscosity can be formulated as given by Miller and Gidaspow [77],

$$\mu_s = -0.188 + 537.42\emptyset \tag{3.38}$$

The drift velocity of the secondary phase $\overline{V_{dr,k}}$ in the Equation 3.36 can be defined such

$$\overline{V_{dr,k}} = \overline{V_{lp}} - \overline{V_m} \tag{3.39}$$

where $\overline{V_{lp}}$ is the slip velocity between two phases and the slip velocity is determined from the equation proposed by Manninen *et al.* [82] as follows

$$\overline{V_{lp}} = \overline{V_l} - \overline{V_p} = \frac{\tau_p(\rho_p - \rho_m)}{f_{drag}\rho_p}\vec{a} \tag{3.40}$$

where τ_p is the particle relaxation time given by

$$\tau_p = \frac{\rho_p {d_p}^2}{18\mu_l} \tag{3.41}$$

and $\vec{a}$ is the secondary phase particle's acceleration expressed as

$$\vec{a} = \left(\overline{V_m}.\nabla\right)\overline{V_m} \tag{3.42}$$

The drag function f_{drag} in Equation 3.40 is given as [83]

$$f_{drag} = \begin{cases} 1 + 0.15Re^{0.687}, & Re \leq 1000 \\ 0.0183Re, & Re > 1000 \end{cases} \tag{3.43}$$

The energy equation for the mixture model can be expressed as

$$\nabla.\left(\sum_{k=1}^{n}\rho_k\emptyset_k\overline{V_k}c_{p,k}\overline{T_m}\right)=\nabla.(k\nabla\overline{T_m}-\rho c_p\overline{V_m'T_m'}) \tag{3.44}$$

For the second two phase formulation, the Eulerian model is considered. In the Eulerian model, the pressure is shared by all phases, while separate continuity, momentum, and energy equations are used for different phases. In the Eulerian model, it should be noted that the solid phase is considered as granular as in the mixture model.

The continuity equations for the liquid and solid phases of the Eulerian model can be expressed as

$$\nabla.\left(\rho_l\emptyset_l\overline{V_l}\right)=0 \tag{3.45}$$

$$\nabla.\left(\rho_p\emptyset_p\overline{V_p}\right)=0 \tag{3.46}$$

$$\emptyset_l+\emptyset_p=1 \tag{3.47}$$

where subscript l and p represent liquid and particle phase, respectively.

The momentum equations for the liquid and solid phases of the Eulerian model can be given as

$$\nabla.\left(\rho_l\emptyset_l\overline{V_lV_l}\right)=-\emptyset_l\nabla\overline{p}+\emptyset_l\nabla.\left[\mu_l\nabla\overline{V_l}+\sum_{k=1}^{n}\rho_k\emptyset_k\overline{V_k'V_k'}\right]+F_d+F_{vm} \tag{3.48}$$

$$\nabla.\left(\rho_p\emptyset_p\overline{V_pV_p}\right)=-\emptyset_p\nabla\overline{p}+\emptyset_p\nabla.\left[\mu_p\nabla\overline{V_p}+\sum_{k=1}^{n}\rho_k\emptyset_k\overline{V_k'V_k'}\right]-F_d-F_{vm}+F_{col} \tag{3.49}$$

where F_d is the drag force vector. F_{vm} and F_{col} are the virtual mass and particle-particle interaction force vectors and assumed to be negligible due to the dilute mixture flow

assumptions [71]. The drag force between the phases can be written as

$$F_d = \beta(\overline{V_{lp}}) \tag{3.50}$$

where β is the friction coefficient given as

$$\beta = \frac{\emptyset_p \emptyset_l \rho_p f_{drag}}{\tau_p} \tag{3.51}$$

The energy equation for the liquid and solid phases of the Eulerian model can be expressed respectively as

$$\nabla.\left(\rho_l \emptyset_l c_{p,l} \overline{V_l T_l}\right) = \nabla.\left(\emptyset_l k_l (\nabla \overline{T_l}\right) - \rho_l \emptyset_l c_{p,l} \overline{V_l' T_l'}) - h_v(\overline{T_l} - \overline{T_p}) \tag{3.52}$$

$$\nabla.\left(\rho_p \emptyset_p c_{p,p} \overline{V_p T_p}\right) = \nabla.\left(\emptyset_p k_p (\nabla \overline{T_p}\right) - \rho_p \emptyset_p c_{p,p} \overline{V_p' T_p'}) - h_v(\overline{T_l} - \overline{T_p}) \tag{3.53}$$

where h_v is the volumetric interphase heat transfer coefficient.

For a single spherical particle dispersion, h_v can be calculated following Kuipers *et al.* [84] as

$$h_v = \frac{6(1-\emptyset_l)}{d_p} h_p \tag{3.54}$$

where h_p is the fluid-particle heat transfer coefficient extracted from the Whitaker empirical correlation [85].

3.3.4. Turbulence Modelling

The k- turbulence model, proposed by Lauder and Spalding [86] is used for calculating the turbulent stress and the turbulent heat flux. This model involves two equations which are turbulent kinetic energy (K) and rate of turbulent kinetic energy dissipation () equations.

The turbulent kinetic energy equation can be written in indicial notation as

$$\frac{\partial(\rho K V_j)}{\partial x_j}=\frac{\partial[\,(\mu+\mu_t/\sigma_K)\,\frac{\partial K}{\partial x_j}]}{\partial x_j}+\mu_t\left(\frac{\partial V_i}{\partial x_j}+\frac{\partial V_j}{\partial x_i}\right)\frac{\partial V_i}{\partial x_i}-\rho\varepsilon \tag{3.55}$$

and the rate of turbulent kinetic energy dissipation can be expressed as

$$\frac{\partial(\rho\varepsilon u_j)}{\partial x_j}=\frac{\partial[\,(\mu+\mu_t/\sigma_\varepsilon)\,\frac{\partial \varepsilon}{\partial x_j}]}{\partial x_j}-\rho C_2\frac{\varepsilon^2}{K}+C_1\frac{\varepsilon}{K}(-\rho\overline{V_j'V_j'}\frac{\partial V_j}{\partial x_i}) \tag{3.56}$$

where σ_K and σ_ε are the turbulent Prandtl numbers for the kinetic energy and dissipation, respectively. The turbulent kinetic energy and dissipation rate are coupled with the governing mass, momentum and energy equations through the turbulent viscosity and turbulent conductivity which are defined by

$$\mu_t=\rho C_\mu\frac{K^2}{\varepsilon} \tag{3.57}$$

$$k_t=\frac{\mu_t c_p}{\sigma_t} \tag{3.58}$$

with C_1= 1.44, C_2= 1.92, C_μ= 0.09, σ_K= 1, σ_ε= 1.3, σ_t= 0.85.

The enhanced wall treatment is also used in turbulence modelling. Bayat and Nikseresht [52] stated that k- turbulence model with near wall modelling gives better results compared to other turbulence models, in turbulent forced convective flow of nanofluids. The enhanced wall treatment is a near-wall modelling method that merges a two layer model with the use of wall functions. In the two layer model, the whole domain is subdivided into a viscosity-affected region and a fully-turbulent region [87].

3.3.5. Numerical Method and Validation

The commercial computational fluid dynamic software package Fluent is used to solve the presented flow problem. The governing equations are solved by the finite volume method which converts the governing equations to discrete algebraic equations, with the use of SIMPLE algorithm for pressure velocity coupling. The second-order

upwind scheme is chosen for discretization of the momentum and energy equations. The User Defined Function (UDF) codes are implemented into the software to calculate the temperature dependent nanofluid properties at every cell. The residuals for the velocity, energy and turbulence components are chosen 10^{-8} for every simulations.

The validation tests for the numerical method are carried out using water as the working fluid for the previously described three physical domains. Also, the mesh structure is chosen according to the dimensionless wall distance y+ value. As recommended by the software package developers, y+ value must be near or smaller than 1 in k- turbulence model with enhanced wall treatment [87]. To catch the proper y+ value, more refined grid structure is applied near the wall. Moreover, rectangular grid type is chosen for the mesh structure. Due to flow symmetry with respect to the tube axis, the half of the flow domain is considered to save computational time. The mesh independency test results with respect to Nusselt number values for fully developed turbulent water flow, are shown in Table 3.1, for all three domains and for Re=30000. In consideration of these results, the 80x800 mesh structure is chosen.

Table 3.1. The mesh independency test for fully developed turbulent water flow at Re=30000.

Domain	**Mesh**	**y+**	**Nu**
Domain 1	20x600	8.45	210.91
	40x800	4.32	209.24
	60x800	1.6	208.112
	80x800	0.8	206.29
	100x800	0.48	206.29
Domain 2	20x600	8.45	210.72
	40x800	4.32	207.8
	60x800	1.6	207
	80x800	0.8	206.27
	100x800	0.48	206.27
Domain 3	20x600	8.45	210.86
	40x800	4.32	209.1
	60x800	1.6	208.07
	80x800	0.8	206.28
	100x800	0.48	206.28

An example of the final mesh structure for Domain 2 is shown in Figure 3.2.

Figure 3.2. The final mesh structure of Domain 2.

The velocity and temperature contours of water flow in Domain 2 at $Re = 30000$ are shown in Figure 3.3.

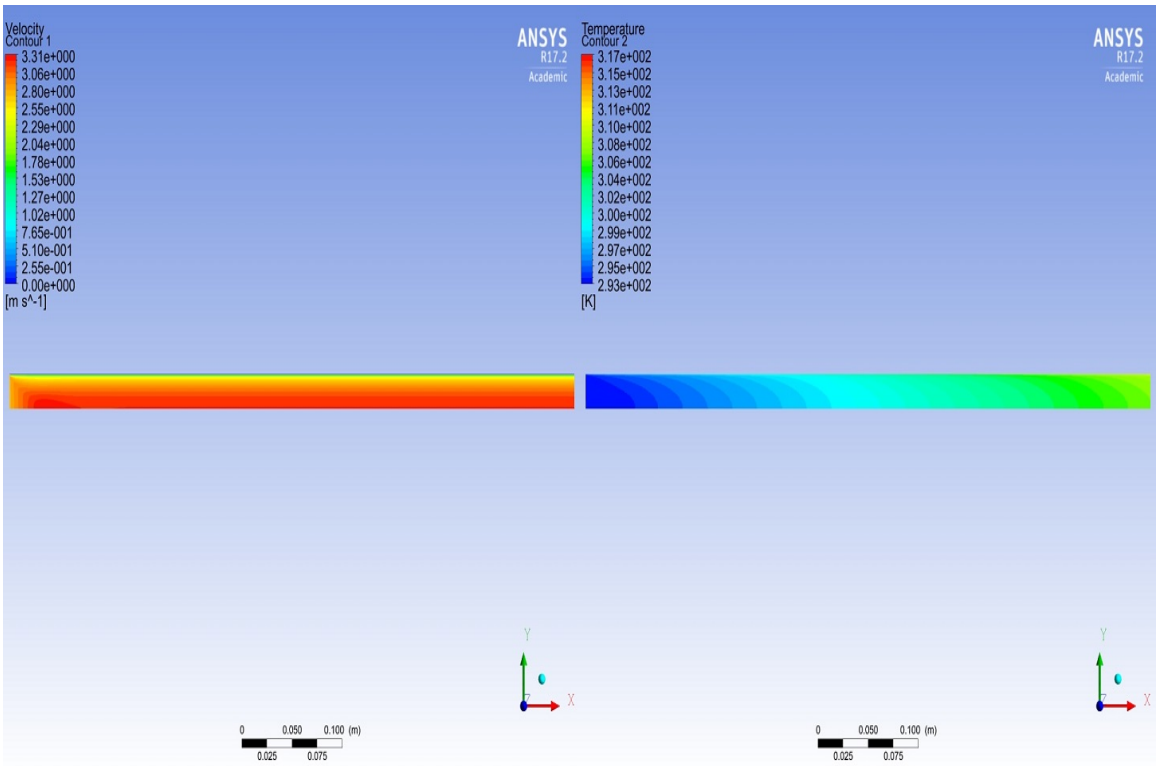

Figure 3.3. The velocity (left) and temperature (right) contours of water flow at Re=30000.

The Nusselt number predictions with respect to Reynolds number are compared with Gnielinski relations and the friction factor predictions are compared with Blasius equation.

The results are displayed in Figure 3.4 and the average errors between Gnielinski and Blasius equations and the simulation results are observed to be 4.24% and 2.46%, respectively.

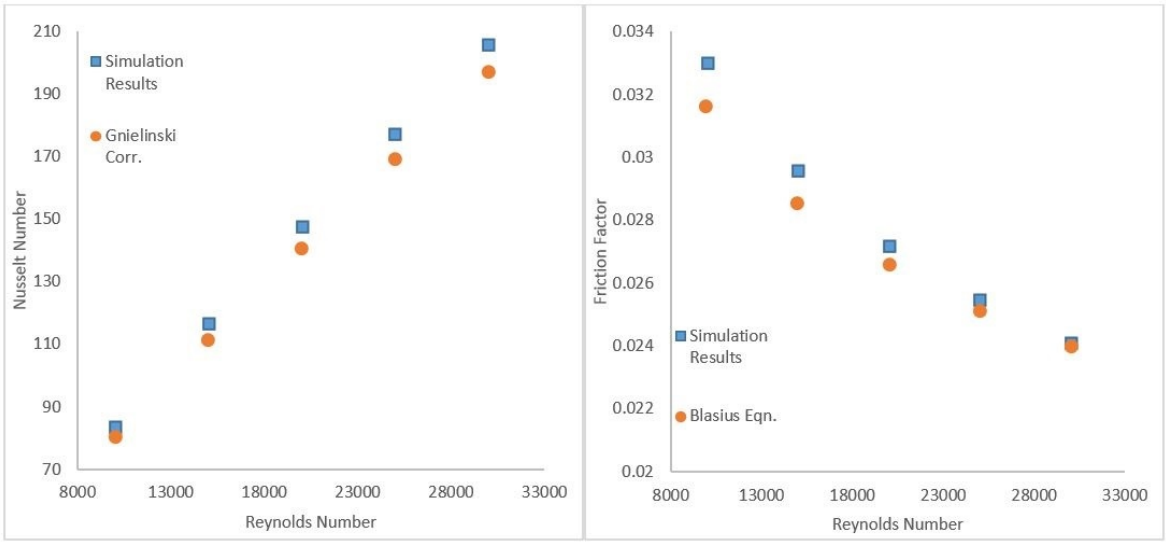

Figure 3.4. The Nusselt number (left) and the friction factor (right) comparison of water simulation for Domain 2.

3.4. Results and Discussions

3.4.1. Flow Model Comparison for Different Volume Concentration Values

In this part, we compare the performance of the single phase and the two phase formulations in the fully developed turbulent flow case with respect to Experiment 1, 4 and Experiment 2 for low and high volume concentration ranges. For volume concentrations less than 0.5%, Experiment 1 and 4's and for volume concentrations above 1%, Experiment 2' s data are considered.

In the simulations of Experiment 1, 20 nm size Al_2O_3/water nanofluid is used. The inlet temperature is taken as 293 K. The bulk temperature of the nanofluid and the Reynolds numbers are extracted from experimental data. The wall heat flux value is chosen according to the bulk temperature value. The volume concentration values are 0.03%, 0.054% and 0.135%. Model 1 and Model 2V are used to define the thermal conductivity and the viscosity of the nanofluid, since Model 1 is the thermal conductivity model derived from the same experiment and Model 2V applies for dilute nanofluids. The Nusselt number results for different volume concentrations are

presented and compared in Figure 3.5

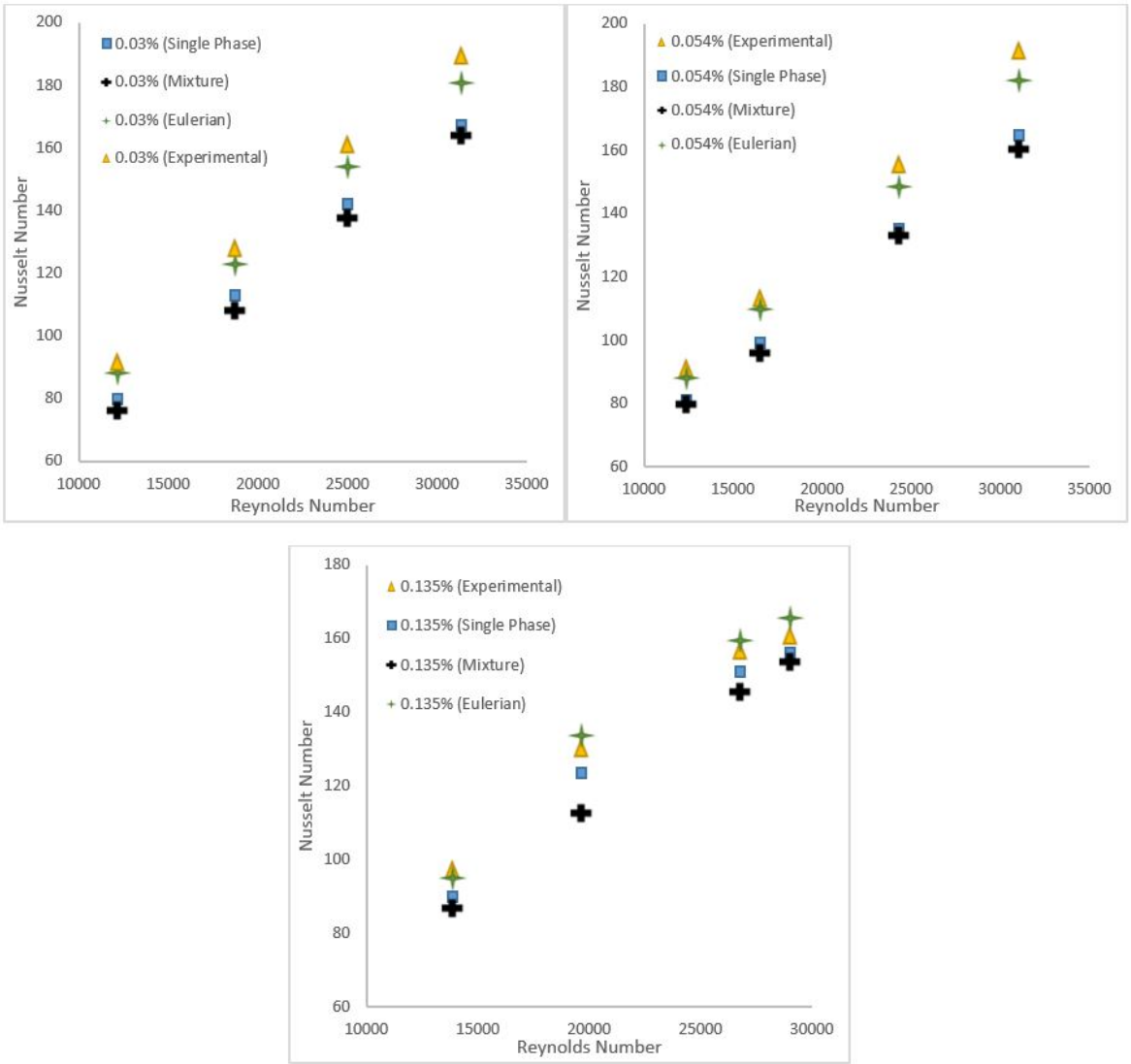

Figure 3.5. The Nusselt number comparison of dilute Al_2O_3/water nanofluid for different flow models ($\emptyset$ =0.03% (top left), $\emptyset$ =0.054% (top right), $\emptyset$ =0.135% (bottom)).

In the simulations of Experiment 4, 40 nm size CuO/water nanofluid is used. The inlet temperature is taken as 293 K. The bulk temperature of the nanofluid and the Reynolds numbers are extracted from experimental data. The wall heat flux value is chosen according to the bulk temperature value. The volume concentration values are 0.015%, 0.118% and 0.236%. Model 1 and Model 2V are used to define the

thermal conductivity and the viscosity of the nanofluid, since Model 1 is the thermal conductivity model derived from the same experiment and Model 2V applies for dilute nanofluids. The Nusselt number results for different volume concentrations are presented and compared in Figure 3.6 .

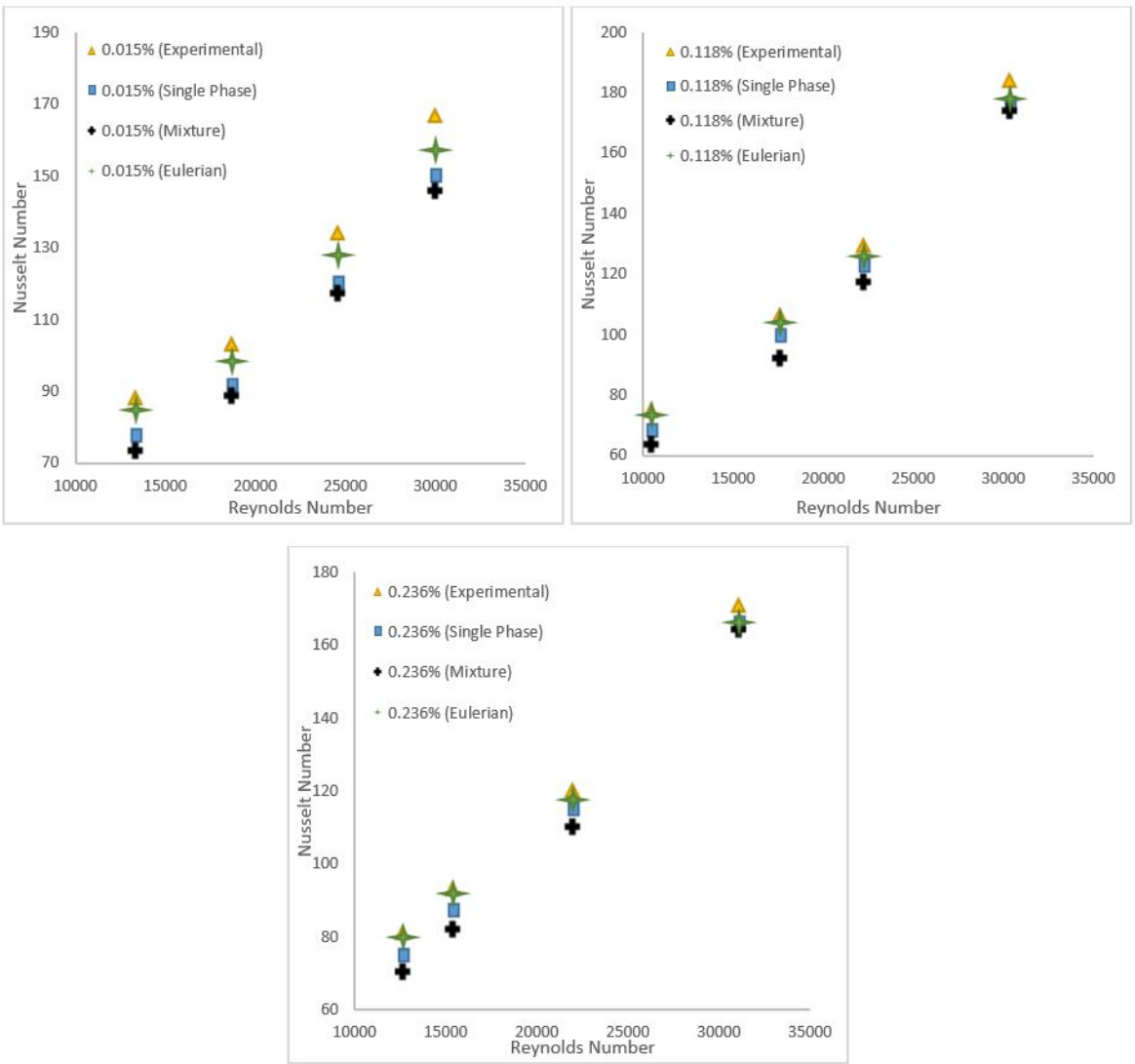

Figure 3.6. The Nusselt number comparison of dilute CuO/water nanofluid for different flow models ($\emptyset$ =0.015% (top left), $\emptyset$ =0.118% (top right), $\emptyset$ =0.236% (bottom)).

In the simulations of Experiment 2, 46 nm size Al_2O_3/water nanofluid is used. The inlet temperature, the bulk temperature and the flow rate values are extracted from

experimental data. The wall heat flux value is chosen according to the experimental current and voltage values. The volume concentration values are 1.8% and 3.6%. Model 2 and Model 1V are used to define the thermal conductivity and the viscosity since these models correspond to the correlations obtained from this experiment. The Nusselt number values for different volume concentrations are presented and compared in Figure 3.7.

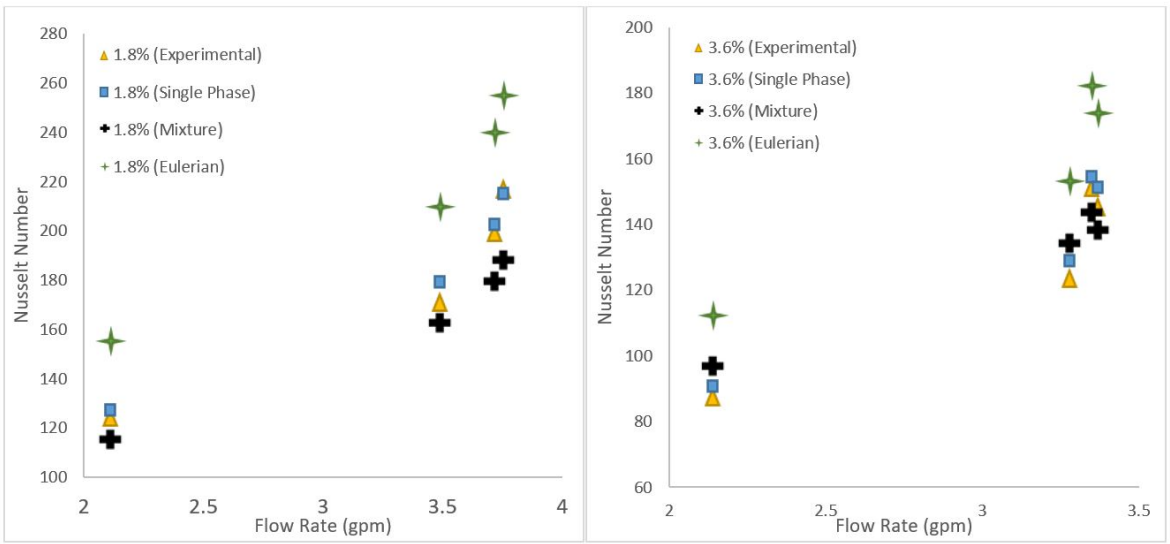

Figure 3.7. The Nusselt number comparison of Al_2O_3/water nanofluid for different flow models ($\emptyset$ =1.8% (left) and $\emptyset$ =3.6% (right)).

The percentage error values for the Nusselt number predictions with respect to Experiment 1, 4 and 2 are shown in Table 3.2, Table 3.3and Table 3.4, respectively.

For the 0.03% volume concentration, it can be understand from Table 3.2, the two phase Eulerian model gives the smallest error values (4.2%-4.7%). The single phase model gives much higher error values compared to the Eulerian model (11.6%-13.3). The two phase mixture model gives maximum error values among the flow models (13.5%-16.6%). The error values of the single phase and the mixture model decrease with increasing Reynolds number. However, the error values of the Eulerian model increase slightly with increasing Reynolds number.

For the 0.054% volume concentration, it is almost the same situation with the 0.03% volume concentration. Only the error values of the flow models are slightly different.

For the 0.135% volume concentration, the error values of the all flow models decreased when compared to the 0.03% and 0.054% volume concentrations. The two phase Eulerian model still gives the least error values.

It can be concluded from Table 3.3, the error values and trends of dilute CuO/ water nanofluid case resemble with dilute Al_2O_3/water nanofluid case. The two phase Eulerian model (1.5%-2.9%) gives the closest results to experimental results while the two phase mixture (3.8%-13.2%) and the single phase (3%-7.4%) models give much higher error values as it is in the dilute Al_2O_3/water case.

For the 1.8% volume concentration, it can be understand from Table 3.4, the singl phase model gives the smallest error values (0.9%-2.7%). The error values of the mixture model (5.1%-13.5%) is higher than the single phase model but lower than the Eulerian model. The error values of the Eulerian model (17.6%-25.1%) is the highest among the tested flow models. It can be seen that the error values of the Eulerian model increased excessively compared to the low concentration cases. Furthermore, the error values of the Eulerian model decrease with increasing Reynolds number contrary to the mixture model. There is no specific trend for the single phase model.

For the 3.6% volume concentration, the order of the error values has not changed. The single phase model still gives the least error values (2.1%-4.2%). The error values of the mixture model decrease with increasing Reynolds number contrary to 1.8% volume concentration case.

It can be observed that for dilute Al_2O_3/water nanofluids with 0.03%, 0.054% and 0.135% volume concentrations, the two phase Eulerian model gives the least error as in the dilute CuO/water nanofluids with 0.015%, 0.118% and 0.236% volume concentrations results. However, for Al_2O_3/water nanofluid with 1.8% and 3.6% vol-

ume concentrations, the single phase model performs much better. This result may be expected, since contrary to low concentrations, at higher concentrations available correlations for thermophysical properties obtained directly from Experiment 2, have been used in the single phase formulation. Despite this fact, an important observation is that the two phase Eulerian model performs well at low concentrations, however at higher concentrations the two-phase mixture model gives much better results than the Eulerian model. It can be observed from the results, the Eulerian model is not recommended for the high concentrations as stated in Behroyan *et al.* [64]. These two phase models are of use in predictions when there are no available correlations obtained from experiments to be applied along with the single phase modelling.

Table 3.2. The Nusselt number percentage error values of dilute $(\emptyset < 0.5\%)$ Al_2O_3/water nanofluid simulations for different flow models.

Experiment	Experiment 1											
Volume Concentration	0.03%				0.054%				0.135%			
Reynolds Number	12100	18700	24950	31350	12350	16450	24300	31020	13800	19600	26750	29000
Single Phase Model	13.3	12.1	11.8	11.6	14.1	13.1	12.9	11.4	7.9	5.2	4.7	3.9
Two Phase Mixture Model	16.6	15.7	14.4	13.5	16.4	15.4	14.4	12.7	13.6	11.1	7.2	4.5
Two Phase Eulerian Model	4.2	4.3	4.3	4.7	3.2	3.3	4.6	5	1.7	2.4	2.5	2.7

Table 3.3. The Nusselt number percentage error values of dilute **($\emptyset < 0.5\%$)** CuO/water nanofluid simulations for different flow models.

Experiment	Experiment 4											
Volume Concentration	0.015%				0.118%				0.236%			
Reynolds Number	13350	18710	24550	29990	10500	17550	22290	30400	12670	15380	21970	31110
Single Phase Model	12.4	11.5	11	10.2	9.1	6.7	5.5	4.2	7.4	6.5	4.6	3
Two Phase Mixture Model	16.8	14.1	13	12.7	15.2	13.4	9.5	5.6	13.2	12.3	8.6	3.8
Two Phase Eulerian Model	4.4	4.6	4.8	5.8	1.8	2.2	2.6	3.2	1.5	1.7	2.3	2.9

Table 3.4. The Nusselt number percentage error values of **($\emptyset > 1\%$)** Al_2O_3/water nanofluid simulations for different flow models.

Experiment	Experiment 2							
Volume Concentration	1.8%				3.6%			
Flow Rate (gpm)	2.111757	3.486365	3.71442	3.756194	2.138405	3.280033	3.367383	3.348142
Reynolds Number	15238	21257	26802	30970	8723	12829	18232	18754
Single Phase Model	1.5	3.4	4.6	6.4	2.9	3.1	3.7	4.2
Two Phase Mixture Model	5.1	6.9	10.1	13.5	10.3	8.3	4.86	5
Two Phase Eulerian Model	25.1	22.7	20.2	17.6	27.8	23.9	19.7	20.4

3.4.2. Comparison of Brownian Motion Effects on the Heat Transfer Enhancement for Laminar and Turbulent Flows

In this subsection, we consider different thermophysical property relations, in the context of single phase modelling, to compare and understand the Brownian motion effects as a mechanism of heat transfer enhancement for laminar and turbulent flows. It was shown in the previous subsection that the single phase model gives accurate results for predicting the experimental findings of Experiment 2, at higher volume concentrations. Therefore we use Experiment 2 data for turbulent flow simulations in this subsection and for laminar flow, Experiment 3 data are considered. Model 1V is used to define the viscosity of nanofluid since this relation is obtained from Experiment 2 and 3 data.

In the simulation of Experiment 3, 50 nm size Al_2O_3/water nanofluid is used. The inlet temperature, the flow rate values and the bulk temperature of nanofluid are extracted from experimental data. The wall heat flux value is chosen according to the experimental current and voltage values. Volume concentration values are 1.32% and 2.76%. The local convective heat transfer coefficient at x=1 m results of different volume concentrations are presented and compared for different thermal conductivity models in Figure 3.8 .

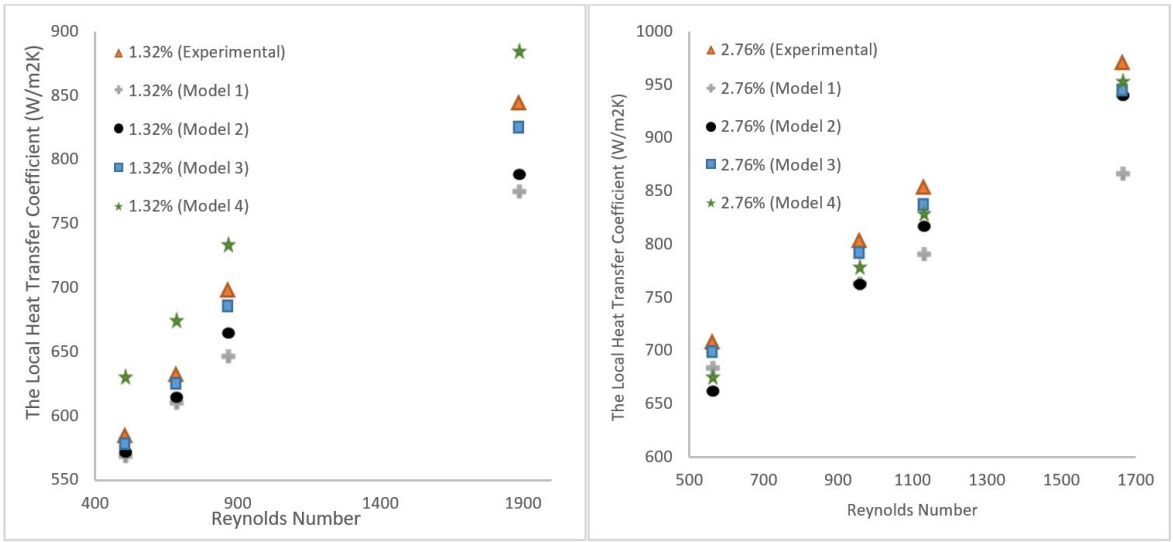

Figure 3.8. The local heat transfer coefficient at x=1 m comparison for different property models ($\emptyset$ =1.32% (left) and $\emptyset$ =2.76% (right)).

The average heat transfer coefficient values are presented for different thermal conductivity models in turbulent nanofluid flow with 1.8% and 3.6% volume concentrations (Experiment 2) in Figure 3.9

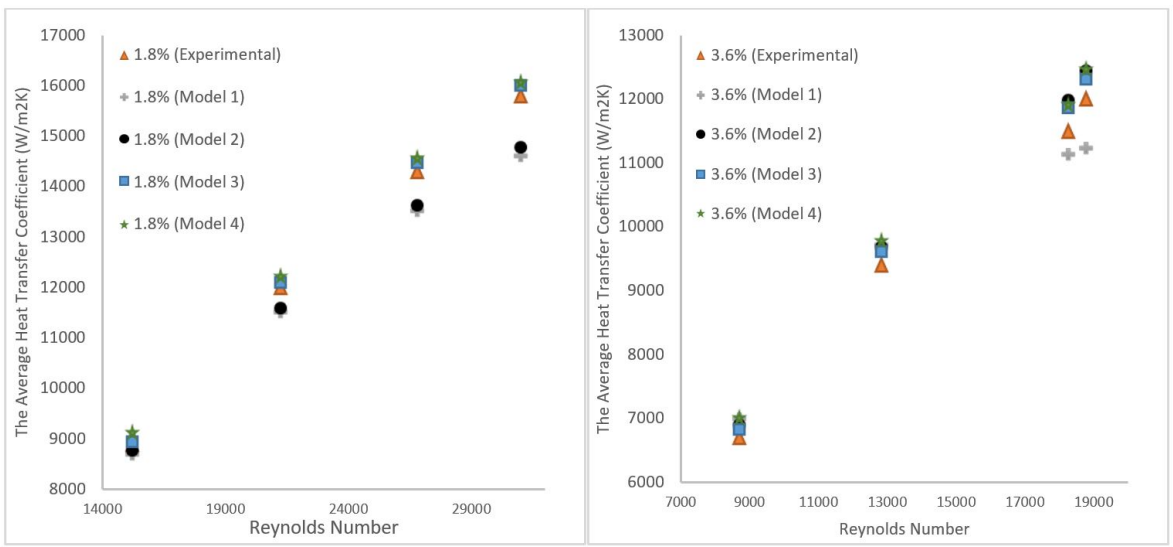

Figure 3.9. The average heat transfer coefficient comparison for different property models ($\emptyset$ =1.8% (left) and $\emptyset$ =3.6% (right)).

The percentage error values for Experiment 2 and 3 are shown in Table 3.5 and Table 3.6, respectively.

For turbulent flow of Al_2O_3/water nanofluid which has 1.8% volume concentration, Model 3 gives the least error values among the tested thermal conductivity models (0.3%-1.3%). Furthermore, Model 4 gives smaller error values except for Re=15238 when compared to Model 1 and Model 2. Moreover, except for Model 4, the error values of the all other models increase with increasing Reynolds number, also, the error values of Model 1 and Model 2 increase more than Model 3.

For turbulent flow of Al_2O_3/water nanofluid which has 3.6% volume concentration, Model 3 gives the least error values as in the 1.8% volume concentration case (2.1%-3.1%). Model 2 gives smaller error values than Model 4 except for Re=18754 contrary to 1.8% volume concentration case. Moreover, except for Model 4, the error values of the all models increase with increasing Reynolds number as in the 1.8% volume concentration case.

For laminar flow of Al_2O_3/water nanofluid which has 1.32% volume concentration, Model 3 gives the smallest error values among the tested models (1.1%-2.3%). All tested model gives higher error values when compared to 1.8% volume concentration turbulent flow case, especially Model 4. However, the trend between the error values and the Reynolds number remains same.

For laminar flow of Al_2O_3/water nanofluid which has 2.76% volume concentration, Model 3 gives the least error values as in the 1.32% volume concentration case (1.3%-2.6%). Moreover, only the error values of Model 4 decrease when compared to 1.32% volume concentration case.

It can be seen that for both laminar and turbulent flows the Chon's model (Model 3) which considers temperature, particle size and Brownian motion effects, gives the least errors. It can be deduced that Brownian motion effect is the one of main mech-

anisms of heat transfer enhancement for both laminar and turbulent flows. It should be noted that Model 2 is found by curve-fitting of experimental results and it is only valid for Experiment 2 and 3. Although Model 4 considers also the Brownian motion effect, it gives higher errors in some conditions. This result may be due to the narrower temperature application range of Model 4 compared to Model 3 and difference in the definitions of the Brownian velocity between Models 3 and 4.

Table 3.5. The average heat transfer coefficient percentage error values of different thermal conductivity models for Experiment 2.

Experiment	Experiment 2 (Turbulent)							
Volume Concentration	1.8%				3.6%			
Reynolds Number	15238	21257	26802	30970	8723	12829	18232	18754
Model 1	2	4	5.3	7.4	3.1	3.6	4.6	6.2
Model 2	1.5	3.4	4.6	6.4	2.9	3.1	3.7	4.2
Model 3	0.3	0.8	1.1	1.3	2.1	2.2	2.6	3.1
Model 4	2.4	2	1.9	1.8	4.5	4.1	3.8	3.6

Table 3.6. The local heat transfer coefficient percentage error values of different thermal conductivity models for Experiment 3.

Experiment	Experiment 3 (Laminar)							
Volume Concentration	1.32%				2.76%			
Reynolds Number	504	685	870	1888	562	957	1131	1666
Model 1	2.9	3.7	7.3	8.3	3.4	5.2	7.6	10.8
Model 2	2.5	3.1	4.8	6.8	3.2	4.5	5.4	6.7
Model 3	1.1	1.3	1.8	2.3	1.3	1.6	2.1	2.6
Model 4	7.7	6.5	5.1	4.7	4.8	3.2	3.1	1.9

3.4.3. Comparison of Pressure Drop Estimations for Laminar and Turbulent Flow of Nanofluid

In this subsection, the pressure drop values for both laminar and turbulent nanofluid flows are compared with experimental data, and the turbulent friction factor values are compared with Equation 3.5 for $Re <= 30000$, with Equation 3.6 for $Re > 30000$ and the laminar friction factor values are compared with 3.4.

The results are displayed in Table 3.7 and Table 3.8. It can be seen that for both laminar and turbulent flows, pressure drop increases with increasing Reynolds number and volume concentration. The pressure drop is more important in turbulent flow when compared with laminar flow. The pressure loss becomes more and more pronounced when the volume concentration and Reynolds number are high as stated in Duangthongsuk and Wongwises [28]. Moreover, the friction factor of Al_2O_3/water nanofluid can be predicted by using well-known equations for both laminar and turbulent flow.

Table 3.7. The pressure drop values and the friction factor comparison for turbulent Al_2O_3/water nanofluid flow.

Experiment	Experiment 2 (Turbulent)							
Volume Concentration	1.8%				3.6%			
Reynolds Number	15238	21258	26802	30971	8724	12829	18232	18754
Pressure Drop (Experiment)	13940.6	37291.7	37395.5	36229.7	18062.5	38160.1	36990.3	35818.2
Pressure Drop (Simulation)	14428.7	37039.4	39186.4	37803.2	18973.4	40182.1	37770.6	36993.8
Friction Factor (Simulation)	0.0263	0.0247	0.0231	0.0219	0.0321	0.0289	0.0259	0.0257
Friction Factor (Theory)	0.0284	0.0261	0.0246	0.0232	0.0326	0.0296	0.0272	0.027

Table 3.8. The pressure drop values and the friction factor comparison for laminar Al_2O_3/water nanofluid flow.

Experiment	Experiment 3 (Laminar)							
Volume Concentration	1.32%				2.76%			
Reynolds Number	504	685	870	1888	562	957	1131	1666
Pressure Drop (Simulation)	254	350.4	451.8	1060.5	627.9	1104.1	1322.9	2030.7
Friction Factor (Simulation)	0.132	0.0972	0.0762	0.0352	0.119	0.0695	0.059	0.0402
Friction Factor (Theory)	0.127	0.0934	0.0735	0.0339	0.113	0.0668	0.0565	0.0384

3.4.4. Comparison of Some Flow and Thermal Parameters for Turbulent Al_2O_3 /water Nanofluid Flow

In this subsection, the wall temperature changes and velocity values along axis of the pipe are investigated and compared each other for 0%, 1.8% and 3.6% volume concentration cases at $Re = 15000$ in Domain 1. The inlet temperature is chosen 293 K. The particle size of the nanoparticles is 46 nm. The best models which give the least error values such as the single phase model with thermal conductivity model 3 and viscosity model 1V for 1.8% and 3.6% volume concentration cases are used in simulations. The wall temperature changes and velocity values along axis of the pipe are shown in Figure 3.10 and Figure 3.11, respectively.

According to the results, it can be seen that the addition of nanoparticles has a significant effect on wall temperature. As the volume concentration of the nanofluid increases, the wall temperature increases. Moreover, the maximum velocity of the flow increases with increasing volume concentration. However, the entrance length which is the distance from the pipe inlet to the fully developed region does not change with volume concentration of the nanofluid.

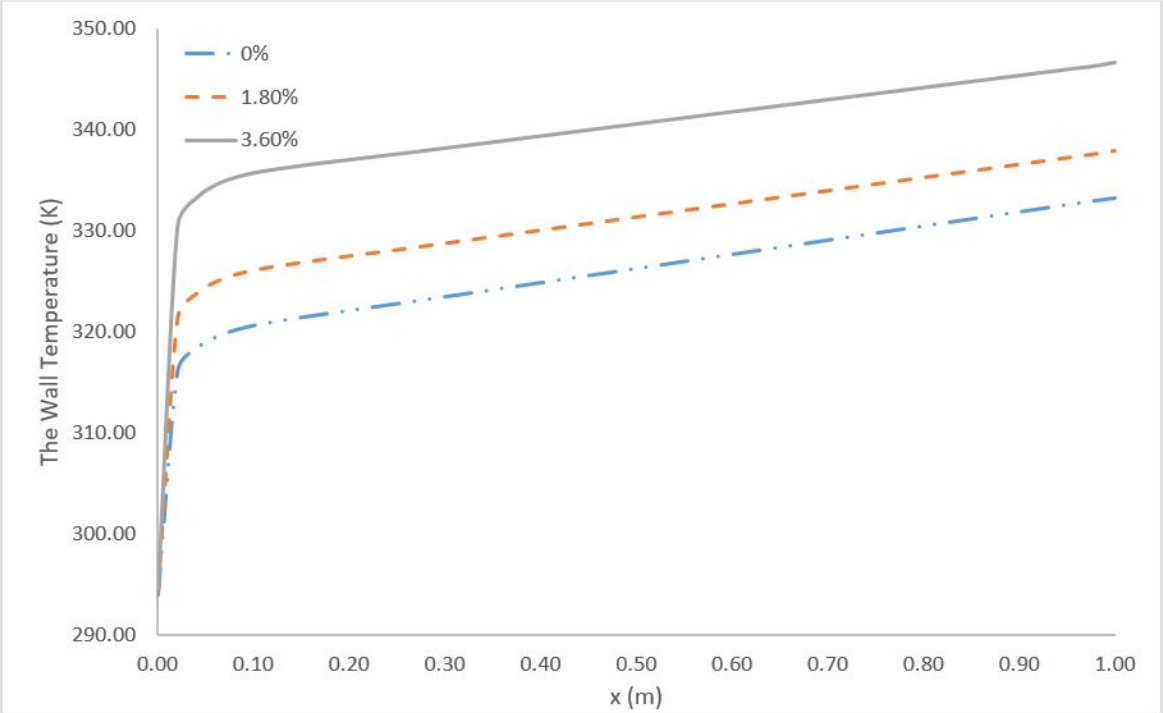

Figure 3.10. The wall temperature changes along the pipe wall for $\emptyset$ =0%, $\emptyset$ =1.8% and $\emptyset$ =3.6% cases at Re=15000.

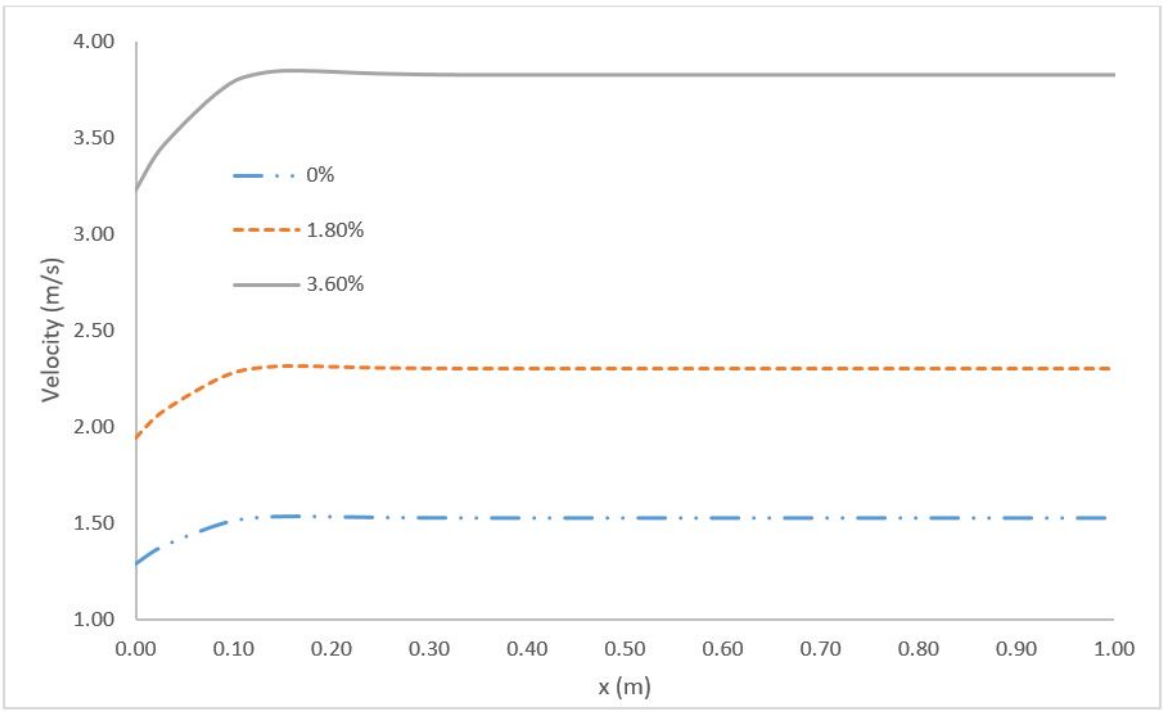

Figure 3.11. The maximum velocity changes along the pipe axis for $\emptyset$ =0%, $\emptyset$ =1.8% and $\emptyset$ =3.6% cases at Re=15000.

3.4.5. Comparison of Heat Transfer Enhancement and Pressure Drop Increase for Laminar and Turbulent Al_2O_3/water Nanofluid Flow

Figure 3.12 shows the ratio of convective heat transfer coefficient of Al_2O_3/ water nanofluid to that of pure water at the same Reynolds number for laminar and turbulent flow conditions. The single phase model results of Al_2O_3/water nanofluids under both laminar and turbulent flow condition with 1.32% and 2.76% volume concentrations are presented. The single phase results using Chon's thermal conductivity model (Model 3) and viscosity model Model 1V which have been shown to give the least errors in these cases, are chosen. Also, the two phase Eulerian model results for Al_2O_3/water nanofluids with 0.135% and 0.03% volume concentrations are presented, since this model predicts better at low concentrations.

For laminar flow of dilute Al_2O_3/water nanofluid, there is no significant difference in terms of heat transfer enhancement and the enhancement does not depend on the Reynolds number. The enhancement is very small. For laminar flow of Al_2O_3/water nanofluids which have volume concentration higher than 1%, the heat transfer enhancement increases with Reynolds number. The enhancement is higher for the nanofluid with higher volume concentration.

For turbulent flow of dilute Al_2O_3/water nanofluid with 0.03% volume concentration, the heat transfer enhancement is same with the laminar case. However, for 0.135% volume concentration case, the enhancement increases compared to the laminar case. Furthermore, the enhancement of both 0.03% and 0.135% volume concentration cases does not change with varying Reynolds number as in the laminar cases. The enhancement is still very small when compared to higher concentration cases. For turbulent flow of Al_2O_3/water nanofluid which have volume concentration higher than 1%, the heat transfer enhancement is slightly more than that of the laminar case for the same volume concentration. Moreover, the enhancement does not show a significant change with increasing Reynolds number contrary to the laminar case.

It can be seen that the convective heat transfer coefficient is higher than that of water for every Reynolds number and volume concentration. The highest h_{nf}/h_{water} is around 1.483 for 2.76% volume concentration at Re=30971. The ratio h_{nf}/h_{water}increases with increasing Reynolds number and volume concentration. However, it can be seen that volume concentration effect is more important than Reynolds number effect. For turbulent and/or the dilute case, the Reynolds number increment has a small effect on the heat transfer enhancement ratio. It can be concluded that the heat transfer enhancement of turbulent nanofluid flow is higher than the enhancement under laminar flow condition for the same volume concentration value.

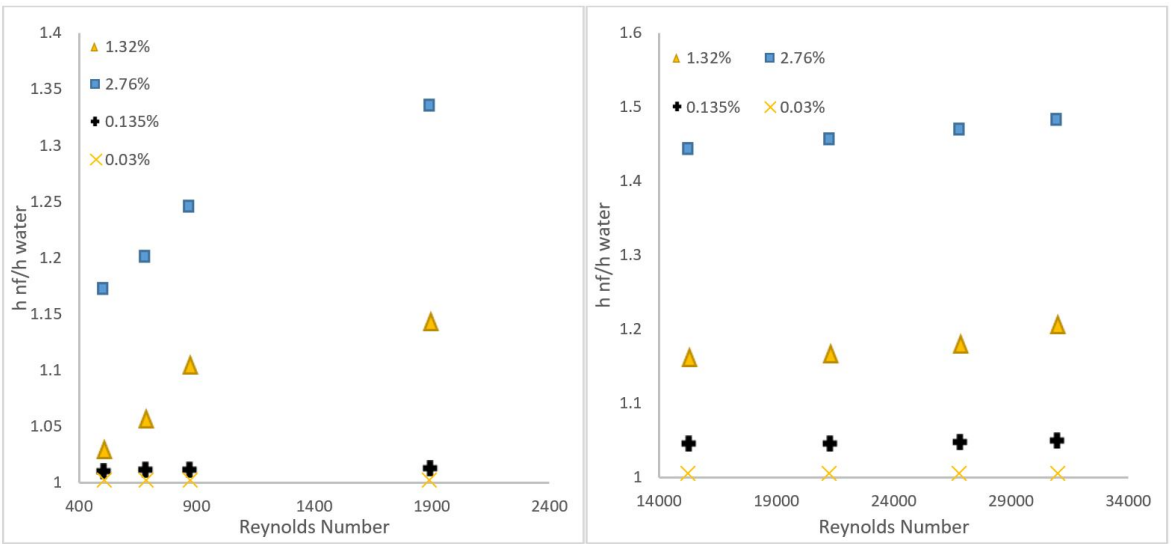

Figure 3.12. The ratio of convective heat transfer coefficient enhancement of Al_2O_3/water nanofluid for laminar (left) and turbulent (right) flow conditions.

Figure 3.13 shows the ratio of the pressure drop of Al_2O_3/water nanofluid to that of pure water at the same Reynolds number for laminar and turbulent flow conditions.

It can be seen that addition of nanoparticles increases the pressure drop for high volume concentrations significantly. However, pressure drop increase is very small for dilute Al_2O_3/water nanofluid. Also, $(\Delta P_{nf}/\Delta P_{water})$ increases with volume concentration and the ratio can be considered independent of the Reynolds number. It is

consistent with the result of Pak and Cho [21] and Williams *et al.* [12]. The increase in the viscosity is mainly responsible for the pressure loss. Therefore, for the same volume concentration the ratio ($\Delta P_{nf}/\Delta P_{water}$) is the same for both laminar and turbulent flow. Also, it is observed that the pressure drop ratio is not affected by the increase in volume concentration in the dilute range.

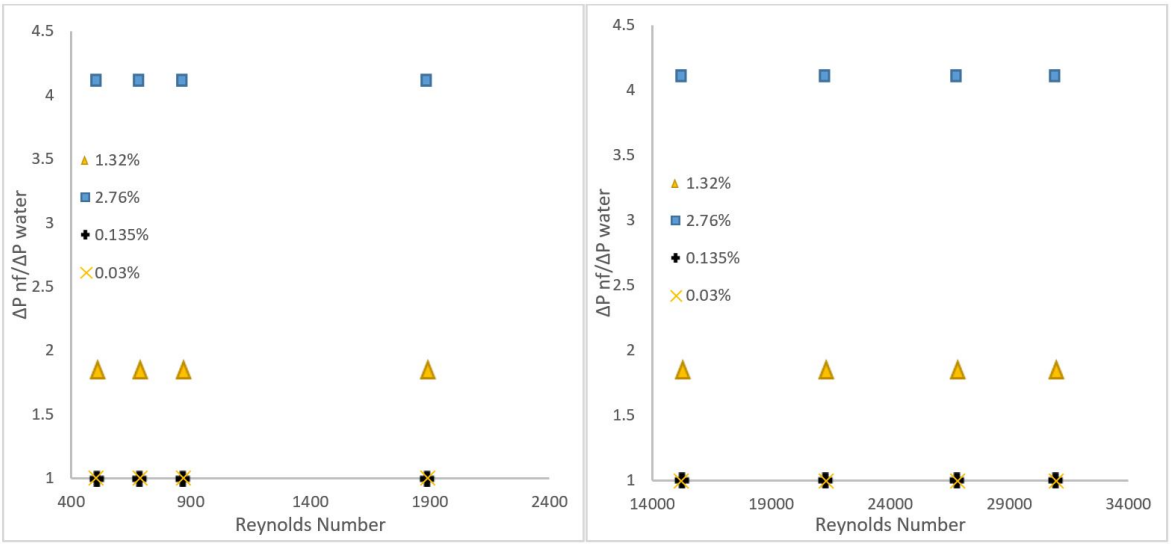

Figure 3.13. The ratio of pressure drop increase of Al_2O_3/water nanofluid for laminar (left) and turbulent (right) flow conditions.

Table 3.9 and Table 3.10 show the ratio of convective heat transfer coefficient enhancement to pressure drop increase in laminar and turbulent flow, respectively. One can understand from this ratio that the case which has the higher ratio is the optimum point for both heat transfer and pressure drop.

It can be seen that the pressure drop increase is higher than the convective heat transfer coefficient enhancement for both laminar and turbulent flow condition and for all volume concentrations except the dilute case, as stated in Sahin *et al.* [31]. Also, for higher volume concentrations, the pressure drop effect is more dominant than heat transfer enhancement for both laminar and turbulent flow. The ratio increases with increasing Reynolds number and decreasing volume concentration. The dilute case is

better than other volume concentrations in terms of pressure loss however the heat transfer enhancement in the dilute case is very low.

For the laminar cases, the ratio increases with increasing Reynolds number for all tested volume concentration cases. Furthermore, it decreases with increasing volume concentration. Therefore, one can expect that the dilute case with higher Reynolds number shows higher ratio. However, the dilute cases is not bright when looking at the heat transfer enhancement. 1.32% volume concentration case is recommended for the application under laminar flow condition among the tested volume concentrations.

For turbulent cases, all trends are similar with the laminar cases. However, the ratio of the turbulent cases is slightly higher than that of the laminar cases for the same volume concentration values. Therefore, 1.32% volume concentration case is the best option when both laminar and turbulent flow cases are considered.

Table 3.9. The ratio of convective heat transfer coefficient enhancement to pressure drop increase comparison of laminar Al_2O_3/water nanofluid flow.

Flow	Laminar											
Volume Concentration	0.135%				1.32%				2.76%			
Reynolds Number	504	685	870	1888	504	685	870	1888	504	685	870	1888
$(h_{nf}/\ h_w)\ /\ (\Delta P_{nf}\ /\ \Delta P_w)$	1.0081	1.0086	1.009	1.01	0.552	0.567	0.592	0.614	0.285	0.292	0.302	0.324

Table 3.10. The ratio of convective heat transfer coefficient enhancement to pressure drop increase comparison of turbulent Al_2O_3/water nanofluid flow.

Flow	Turbulent											
Volume Concentration	0.135%				1.32%				2.76%			
Reynolds Number	15238	21257	26802	30970	15238	21257	26802	30970	15238	21257	26802	30970
$(h_{nf}/\ h_w)\ /\ (\Delta P_{nf}\ /\ \Delta P_w)$	1.0438	1.0441	1.0461	1.048	0.624	0.627	0.634	0.648	0.35	0.354	0.357	0.36

3.4.6. Comparison of Simulation results of Turbulent Al_2O_3/water Nanofluid Flow with Proposed Correlations and Chilton-Colburn Analogy

Different correlations have been proposed in the literature for predicting Nusselt number in turbulent Al_2O_3/water nanofluid flow. Figure 3.14 compares simulation results of Experiment 2 with the results obtained from correlations proposed by Pak and Cho [21] and Maiga *et al.* [11] for 1.8% and 3.6% volume concentrations. It is observed that for both volume concentrations, simulation results are in good agreement with Pak and Cho correlation, although there are small deviations at some points due to the difference in the Prandtl number range, while Maiga's correlation overpredicts the Nusselt number. It should be noted that Pak and Cho's correlation is purely experimental, however Maiga's correlation is found by numerical simulations.

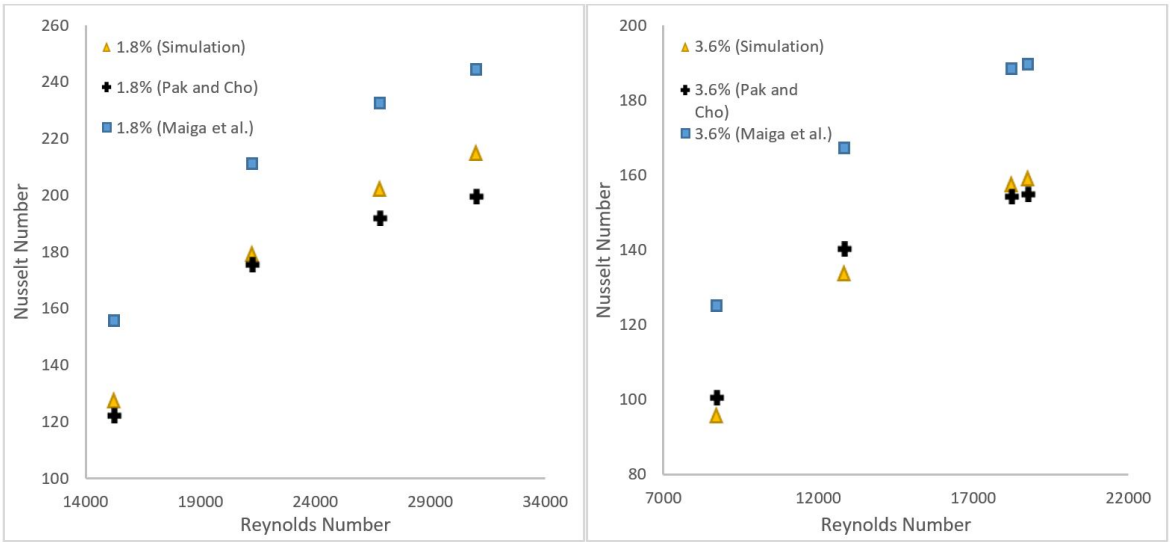

Figure 3.14. Comparison of the Nusselt number results with existing correlations for nanofluids at $\emptyset$ =1.8% (left) and $\emptyset$ =3.6% (right) volume concentration.

In this section, the suitability of the Chilton-Colburn analogy for nanofluids has also been investigated. The friction factor and the Nusselt number results for turbulent Al_2O_3/water nanofluid flow are used with chosen Reynolds number and Prandtl number values to check whether the simulation results fits to Chilton-Colburn analogy (Equation 3.17). The results are shown in Table 3.11.

According to the results, it has been observed that turbulent Al_2O_3/water nanofluid flow does not conform to the Chilton-Colburn analogy. Chilton and Colburn have built their analogy on the experimental results of some liquids in the literature. Therefore, the difference in results may be due to the fact that the flow and thermal properties of nanofluids are not similar with conventional fluids.

Table 3.11. Chilton-Colburn Analogy for Al_2O_3/water nanofluid.

Flow	Turbulent											
Volume Concentration	0.135%				1.8%				3.6%			
Reynolds Number	13800	19600	26750	29000	15238	21257	26802	30970	8723	12829	18232	18754
Prandtl Number	3.21	3.31	3.21	3.31	6.86	8.45	6.86	5.79	11.27	11.82	7.86	8.17
Nusselt Number	95.1	133.5	159.5	165.4	132.4	186.3	214.4	229.6	94.4	133.3	163.7	158.3
Friction Factor	0.0332	0.0294	0.0266	0.0259	0.0263	0.0247	0.0231	0.0219	0.0321	0.0289	0.0259	0.0257
$StPr^{2/3}$	0.0047	0.0046	0.004	0.0038	0.0046	0.0043	0.0042	0.0041	0.0048	0.0046	0.0045	0.0042
$f/8$	0.0041	0.0037	0.0033	0.0032	0.0032	0.003	0.0029	0.0027	0.004	0.0036	0.0032	0.0032

4. CONCLUSION AND FUTURE WORK

4.1. Conclusion

In the present paper, steady state turbulent forced convection of Al_2O_3/water nanofluid inside a pipe has been investigated numerically. The main aim of this study were to develop a numerical procedure which predicts the flow and heat transfer characteristics of the nanofluid accurately for a wide range of volume concentration and Reynolds number. Therefore, a lot of flow and property models were tried and the results were compared with experimental works. The single phase, two phase mixture and Eulerian models have been used and compared each other to obtain a numerical procedure with high accuracy. Different thermophysical relation models have been tried and compared to improve the accuracy of the single phase model prediction. Moreover, the laminar flow of Al_2O_3/water nanofluid was added to compare it with turbulent heat transfer and pressure drop behavior of the Al_2O_3/water nanofluid.

It has been observed that the two phase Eulerian model performs best at low concentrations while the two phase mixture model gives better predictions at higher concentrations compared to the Eulerian model. As expected, the single phase model gives the least errors when direct correlations for thermophysical properties are available from experiments.

It has been shown that the Brownian effect is one of the main mechanisms for the heat transfer enhancement in both laminar and turbulent flow.

Results showed that nanoparticles addition increases the heat transfer rate as well as the pressure drop. Moreover, heat transfer and pressure drop for the nanofluid increases with increasing volume concentration and Reynolds number, as observed in the experiments. The highest heat transfer rate and pressure drop values have been detected at the highest Reynolds number and volume concentration. However, the pressure drop increase for the nanofluid with respect to base fluid ($\Delta P_{nf}/\Delta P_{water}$) is

independent of the Reynolds number and it only increases with increasing volume concentration. Also, the heat transfer enhancement (h_{nf}/ h_{water})increases with increasing Reynolds number and volume concentration. However, the Reynolds number increment has a small effect on the heat transfer enhancement for turbulent flows and/or dilute suspensions.The heat transfer enhancement in turbulent flow condition is higher than the enhancement in laminar flow condition for the same volume concentration value. Therefore, at a given concentration, the ratio of heat transfer enhancement to pressure drop increase value ((h_{nf} / h_{water}) / (ΔP_{nf} / ΔP_{water})) is higher in turbulent flow condition compared to laminar flow condition for both dilute and high concentration cases. It can be concluded that using nanofluids in turbulent flow condition is more effective than in laminar flow condition case for the same volume concentration.

The following can be considered as the main results of this study:

- When the proper thermophysical property models are found, the single phase model is sufficient for a wide range of volume concentrations and Reynolds number.
- Two phase Eulerian model performs better at low concentrations, two phase mixture model is more accurate at higher concentrations. However, the Eulerian model is not recommended for higher concentrations.
- Although the property models are not used in the two phase modelling, the computational time and the error values of the two phase models are higher than the single phase model.
- Brownian motion is effective in heat transfer enhancement for both laminar and turbulent nanofluid flow.
- Heat transfer enhancement is higher in turbulent flow compared to laminar flow at a given volume concentration
- Pressure drop increase ratio depends on volume concentration, and not on Reynolds number.
- The ratio of heat transfer to pressure drop increase is higher in turbulent flow compared to laminar flow.

4.2. Contribution and Future Work

Heat transfer and pressure drop characteristics of a working fluid are a fundamental issue for thermal systems. The optimal design and safe operation are strongly depend on these characteristics. This thesis has contributed to analyze the heat transfer and flow behaviors of nanofluid accurately without doing experimental works. Moreover, it was investigated that which CFD model is more suitable for different conditions. It has been found in the literature research that there is still uncertainty about this matter. The results show that the single phase model can be used to predict the heat transfer and flow behavior of nanofluid, especially for the higher volume concentrations, if the suitable thermophysical property models can be found. However, it is difficult to find a suitable models among many models for many kinds of nanofluids and applications. Therefore, the importance of the two phase modelling comes forth at this point. When the two phase models are compared with each other, the Eulerian model is the best model at low concentrations, however, the mixture model becomes better than the Eulerian model as the volume concentration increases. Furthermore, the Eulerian model predicts the forced convection heat transfer of the turbulent nanofluid flow inaccurately.

The different UDF codes have been developed to determine the thermophysical property models of a nanofluid (see Appendix A). This codes can be used and implemented to Ansys-Fluent software for modelling.

This study can be used as a reference for the selection of the flow and property models in numerical application and can be used to determine the best operating point of thermal systems that use nanofluids.

The two phase granular model can be improved for future work. Because there are different solid phase viscosity models available in the literature. In this study, only the Miller and Gidaspow model is used to define solid phase. Moreover, some articles stated that Eulerian Lagrangian model is better than other flow models in terms of heat transfer prediction. However, since the number of these articles is low, more work must

be done to trust this flow model. Furthermore, there is a new type of nanofluids that are called 'hybrid' in the literature. The hybrid nanofluids are obtained by mixing different type of nanoparticles in a base fluid. The heat transfer and flow behavior of hybrid nanofluids may be investigated numerically when a sufficient number of experimental works are conducted in this subject.

REFERENCES

1. Das, S. K., S. U. Choi, W. Yu and T. Pradeep, *Nanofluids: Science and Technology*, John Wiley & Sons, Inc., Hoboken, NJ, USA, 2008.

2. Maxwell, J. C., *A Treatise on Electricity and Magnetism*, Oxford University Press, Cambridge, U.K., 1904.

3. Hamilton, R. I. and O. K. Crosser, "Thermal Conductivity of Heterogeneous Two Component Systems", *Industrial and Engineering Chemistry Fundamentals*, Vol. 1, pp. 187–191, 1962.

4. Yu, W. and S. U. S. Choi, "The Role of Interfacial Layers in the Enhanced Thermal Conductivity of Nanofluids: A Renovated Maxwell Model", *Journal of Nanoparticle Research*, Vol. 5, pp. 167–171, 2003.

5. Koo, J. and C. Kleinstreuer, "A New Thermal Conductivity Model for Nanofluids", *Journal of Nanoparticle Research*, Vol. 6, pp. 577–588, 2004.

6. Chon, C. H., K. D. Kihm, S. P. Lee and S. U. S. Choi, "Empirical Correlation Finding the Role of Temperature and Particle Size for Nanofluid (Al_2O_3) Thermal Conductivity Enhancement", *Applied Physics Letters*, Vol. 87, pp. 1531071–1531073, 2005.

7. Patel, H., T. Sundarajan, T. Pradeep, A. Dasgupta, N. Dasgupta and K. Das, "A Micro-Convection Model for Thermal Conductivity of Nanofluids", *Journal of Physics*, Vol. 65, pp. 863–869, November 2005.

8. Jang, S. P. and S. U. S. Choi, "Role of Brownian Motion in the Enhanced Thermal Conductivity of Nanofluids", *Applied Physics Letters*, Vol. 84, pp. 4316–4318, 2004.

9. Li, C. and G. Peterson, "Mixing Effect on the Enhancement of the Effective Ther-

mal Conductivity of Nanoparticle Suspensions (Nanofluids)", *International Journal of Heat and Mass Transfer*, Vol. 50, pp. 4668–4677, 2007.

10. Evans, W., J. Fish and P. Keblinski, "Role of Brownian Motion Hydrodynamics on Nanofluid Thermal Conductivity", *Applied Physics Letters*, Vol. 88, pp. 093116–3, 2006.

11. Maiga, S. E. C., C. T. Nguyen, N. Galanis and G. Roy, "Heat Transfer Behaviours of Nanofluids in a Uniformly Heated Tube", *Superlattices and Microstructures*, Vol. 35, pp. 543–557, 2004.

12. Williams, W., J. Buongiorno and L. Hu, "Experimental Investigation of Turbulent Convective Heat Transfer and Pressure Loss of Alumina/Water and Zirconia/Water Nanoparticle Colloids (Nanofluids) in Horizontal Tubes", *Journal of Heat Transfer*, Vol. 130, pp. 042412–1, April 2008.

13. Mintsa, H. A., G. Roy, C. T. Nguyen and D. Doucet, "New Temperature Dependent Thermal Conductivity Data for Water-based Nanofluids", *International Journal of Thermal Sciences*, Vol. 48, pp. 363–371, 2009.

14. Corcione, M., "Empirical Correlating Equations for Predicting the Effective Thermal Conductivity and Dynamic Viscosity of Nanofluids", *Energy Conversion and Management*, Vol. 52, pp. 789–793, 2011.

15. Einstein, A., "Eine neue Bestimmung der Molekuldimensionen", *Annalen der Physik*, pp. 289–306, 1906.

16. Brinkman, H. C., "The Viscosity of Concentrated Suspensions and Solutions", *The Journal of Chemical Physics*, Vol. 20, pp. 571–581, 1952.

17. Batchelor, G. K., "Effect of Brownian-motion on Bulk Stress in a Suspension of Spherical-particles", *Journal of Fluid Mechanics*, Vol. 83, pp. 97–117, 1977.

18. Nguyen, C. T., F. Desgranges, G. Roy, N. Galanis, T. Mare, S. Boucher and et al., "Temperature and Particle-size Dependent Viscosity Data for Water-based Nanofluids-Hysteresis Phenomenon", *International Journal of Heat and Fluid Flow*, Vol. 28, pp. 1492–1506, 2007.

19. Masuda, H., A. Ebata, K. Teramae and N. Hishinuma, "lteration of Thermal Conductivity and Viscosity of Liquid by Dispersing Ultra Fine Particles", *Netsu Bussei*, Vol. 4, pp. 227–233, 1993.

20. Wang, X., X. Xu and S. U. S. Choi, "Thermal Conductivity of Nanoparticle–fluid Mixture", *Journal of Thermophysics and Heat Transfer*, Vol. 13, pp. 474–480, 1999.

21. Pak, B. C. and Y. I. Cho, "Hydrodynamic and Heat Transfer Study of Dispersed Fluids with Submicron Metallic Oxide Particles", *Experimental Heat Transfer*, Vol. 11, pp. 151–170, 1998.

22. Abu-Nada, E., "Effects of Variable Viscosity and Thermal Conductivity of CuO-Water Nanofluid on Heat Transfer Enhancement in Natural Convection: Mathematical Model and Simulation", *International Journal of Heat and Fluid Flow*, Vol. 30, pp. 679–690, 2009.

23. Duangthongsuk, W. and S. Wongwises, "Measurement of Temperature-dependent Thermal Conductivity and Viscosity of TiO_2/water Nanofluids", *Experimental Thermal and Fluid Science*, Vol. 33, pp. 706–714, 2009.

24. Masoumi, N., N. Sohrabi and A. Behzadmehr, "A New Model for Calculating the Effective Viscosity of Nanofluids", *Journal of Physics D: Applied Physics*, Vol. 42, 2009.

25. Xuan, Y. and Q. Li, "Investigation on Convective Heat Transfer and Flow Features of Nanofluids", *Journal of Heat Transfer*, Vol. 125, pp. 151–155, 2003.

26. Dittus, F. and L. Boelter, "Heat Transfer in Automobile Radiators of the Tubular Type", *International Communications in Heat and Mass Transfer*, pp. 3–22, 1985.

27. Rea, U., T. McKrell, L. Hu and J. Buongiorno, "Laminar Convective Heat Transfer and Viscous Pressure Loss of Alumina–water and Zirconia–water Nanofluids", *International Journal of Heat and Mass Transfer*, Vol. 52, pp. 2042–2048, 2009.

28. Duangthongsuk, W. and S. Wongwises, "An Experimental Study on the Heat Transfer Performance and Pressure Drop of TiO_2-water Nanofluids Flowing Under a Turbulent Flow Regime", *Experimental Thermal and Fluid Science*, Vol. 53, pp. 334–344, 2010.

29. Fotukian, S. and M. Esfahany, "Experimental Investigation of Turbulent Convective Heat Transfer of Dilute c-Al_2O_3/water Nanofluid Inside a Circular Tube", *International Journal of Heat and Fluid Flow*, Vol. 31, pp. 606–612, 2010.

30. Fotukian, S. and M. Esfahany, "Experimental Study of Turbulent Convective Heat Transfer of Dilute CuO/water Nanofluid Inside a Circular Tube", *International Communications in Heat and Mass Transfer*, pp. 214–219, 2010.

31. Sahin, B., G. Gültekin, E. Manay and S. Karagoz, "Experimental Investigation of Heat Transfer and Pressure Drop Characteristics of Al_2O_3-water Nanofluid", *Experimental Thermal and Fluid Science*, Vol. 50, pp. 21–28, 2013.

32. Amrollahi, A., A. M. Rashidi, R. Lotfi, M. E. Meibodi and K. Kashefi, "Convection Heat Transfer of Functionalized MWNT in Aqueous Fluids in Laminar and Turbulent Flow at the Entrance Region", *International Communications in Heat and Mass Transfer*, Vol. 37, pp. 717–723, 2010.

33. Chavan, D. and A. T. Pise, "Experimental Investigation of Convective Heat Transfer Agumentation using Al_2O_3/water Nanofluid in a Circular Pipe", *Heat and Mass Transfer*, Vol. 51, pp. 1237–1246, 2015.

34. Heyhat, M. M., F. Kowsary, A. M. Rashidi, S. A. V. Esfehani and A. Amrollahi, "Experimental Investigation of Turbulent Flow and Convective Heat Transfer Characteristics of Alumina Water Nanofluids in Fully Developed Flow Regime", *International Communications in Heat and Mass Transfer*, Vol. 39, pp. 1272–1278, 2012.

35. Kayhani, M. H., H. Soltanzadeh, M. M. Heyhat, M. Nazari and F. Kowsary, "Experimental study of convective heat transfer and pressure drop of TiO_2/water Nanofluid", *International Communications in Heat and Mass Transfer*, Vol. 39, pp. 456–462, 2012.

36. Wusiman, K., H. Chung, N. MD, A. Handry, Y. Eom, J. Kim and H. Jeong, "Heat Transfer Characteristics of Nanofluid Through Circular Tube", *Journal of Central South University of Technology*, Vol. 20, pp. 142–148, 2013.

37. Hojjat, M., S. G. Etemad, R. Bagheri and J. Thibault, "Turbulent Forced Convection Heat Transfer of non-Newtonian Nanofluids", *Experimental Thermal and Fluid Science*, Vol. 35, pp. 1351—-1356, 2011.

38. Azmi, W. H., K. V. Sharma, P. K. Sarma, R. Mamat, S. Anuar and V. D. Rao, "Experimental Determination of Turbulent Forced Convection Heat Transfer and Friction Factor with SiO_2 Nanofluid", *Experimental Thermal and Fluid Science*, Vol. 51, pp. 103—-111, 2013.

39. Merilainen, A., A. Seppala, K. Saari, J. Seitsonen, J. Ruokolainen, S. Puisto, N. Rostedt and T. Ala-Nissila, "Influence of Particle Size and Shape on Turbulent Heat Transfer Characteristics and Pressure Losses in Water-based Nanofluids", *International Journal of Heat and Mass Transfer*, Vol. 61, pp. 439—448, 2013.

40. Anoop, K., T. Sundararajan and S. K. Das, "Effect of Particle Size on the Convective Heat Transfer in Nanofluid in the Developing Region", *International Journal of Heat and Mass Transfer*, Vol. 52, pp. 2189–2195, 2009.

41. Wen, D. and Y. Ding, "Experimental Investigation into Convective Heat Transfer of Nanofluids at the Entrance Region Under Laminar Flow Conditions", *International Journal of Heat and Mass Transfer*, Vol. 47, pp. 5181–5188, 2004.

42. Yang, Y., Z. G. Zhang, E. A. Grulke, W. B. Anderson and G. Wu, "Heat Transfer Properties of Nanoparticle-in-fluid Dispersions (Nanofluids) in Laminar Flow", *International Journal of Heat and Mass Transfer*, Vol. 48, pp. 1107–1116, 2005.

43. Zeinali, S. H., S. G. Etemad and M. N. Esfahany, "Experimental Investigation of Oxide Nanofluids Laminar Flow Convective Heat Transfer", *International Communications in Heat and Mass Transfer*, Vol. 33, pp. 529–535, 2006.

44. Sultan, K. F., *An Investigation in to Heat Transfer and Flow Of Nanofluids in Circular Tube*, Ph.D. Thesis, University of Technology, Iraq, 2012.

45. Sajadi, A. R. and M. R. Kazemi, "Investigation of Turbulent Convective Heat Transfer and Pressure Drop of TiO_2/water Nano fluid in Circular Tube", *International Communications in Heat and Mass Transfer*, Vol. 38, pp. 1474–1478, 2011.

46. Sundar, L. S., M. T. Naik, K. V. Sharma, M. K. Singh and T. C. S. Reddy, "Experimental Investigation of Forced Convection Heat Transfer and Friction Factor in a Tube with Fe_3O_4 Magnetic Nanofluid", *Experimental Thermal and Fluid Science*, Vol. 37, pp. 65–71, 2012.

47. Nasiri, M., S. G. Etemad and R. Bagheri, "Experimental Heat Transfer of Nanofluid Through an Annular Duct", *International Communications in Heat and Mass Transfer*, Vol. 38, pp. 958–963, 2011.

48. Ding, Y. L., H. S. Chen, Y. R. He, A. Lapkin, M. Yeganeh, L. Siller and et al., "Forced Convective Heat Transfer of Nanofluids", *Advanced Powder Technology*, Vol. 18, pp. 813–824, 2007.

49. Hwang, K. S., S. P. Jang and S. U. S. Choi, "Flow and Convective Heat Transfer

Characteristics of Water-based Al_2O_3 Nanofluids in Fully Developed Laminar Flow Regime", *International Journal of Heat and Mass Transfer*, Vol. 52, pp. 193–199, 2009.

50. Namburu, P. K., D. K. Das, K. M. Tanguturi and R. S. Vajjha, "Numerical Study of Turbulent Flow and Heat Transfer Characteristics of Nanofluids Considering Variable Properties", *International Journal of Thermal Sciences*, Vol. 48, pp. 290–302, 2009.

51. Gnielinski, V., "New Equations for Heat and Mass Transfer in Turbulent Pipe and Channel Flow", *International Chemical Engineering*, Vol. 16, pp. 359–368, 1976.

52. Bayat, J. and A. Nikseresht, "Thermal Performance and Pressure Drop Analysis of Nanofluids in Turbulent Forced Convective Flows", *International Journal of Thermal Sciences*, Vol. 60, pp. 236–243, 2012.

53. Kumar, P., "A CFD Study of Heat Transfer Enhancement in Pipe Flow with Al_2O_3 Nanofluid", *International Journal of Mechanical, Aerospace, Industrial, Mechatronic and Manufacturing Engineering*, Vol. 5, pp. 1850–1854, 2011.

54. Hatami, F. and F. Okhovati, "Analysis of Turbulent Flow of Nanofluids in a Pipe", *European Online Journal of Natural and Social Sciences*, Vol. 3, pp. 72–85, 2011.

55. Shedid, M. H., "Computational Heat Transfer for Nanofluids through an Annular Tube", *Proceedings of the International Conference on Heat Transfer and Fluid Flow*, Vol. 206, 2014.

56. Moraveji, M. K. and A. R. Behesti, "CFD Study of the Turbulent Forced Convective Heat Transfer of Non-Newtonian Nanofluid", *Iranian Journal of Chemical Engineering*, Vol. 11, pp. 92–102, 2014.

57. Kumar, P. and R. Ganesan, "A CFD Study of Turbulent Convective Heat Transfer Enhancement in Circular Pipeflow", *International Journal of Mathematical, Com-*

putational, Physical, Electrical and Computer Engineering, Vol. 6, pp. 909–916, 2012.

58. Aghai, A., G. A. Sheikhzadeh, M. Dastmalchi and H. Forozande, "Numerical Investigation of Turbulent Forced-convective Heat Transfer of Al_2O_3–water Nanofluid with Variable Properties in Tube", *Ain Shams Engineering Journal*, Vol. 6, pp. 577–585, 2015.

59. Hussein, A. M., R. A. Bakar, K. Kadirgama and K. V. Sharma, "Simulation Study of Turbulent Convective Heat Transfer Enhancement in Heated Tube Flow using TiO_2-water Nanofluid", *2nd International Conference on Mechanical Engineering Research*, Vol. 50, 2013.

60. Özerinç, S., A. G. Yazıcıoğlu and S. Kakaç, "Numerical Analysis of Laminar Forced Convection with Temperature-dependent Thermal Conductivity of Nanofluids and Thermal Dispersion", *International Journal of Thermal Sciences*, Vol. 62, pp. 138–148, 2012.

61. Azimi, S. S. and M. Kalbasi, "Numerical Study of Dynamic Thermal Conductivity of Nanofluid in the Forced Convective Heat Transfer", *Applied Mathematical Modelling*, Vol. 38, pp. 1373–1384, 2014.

62. Behzadmehr, A., M. Saffar-Avval and N. Galanis, "Prediction of Turbulent Forced Convection of a Nanofluid in a Tube with Uniform Heat Flux using a Two Phase Approach", *International Journal of Heat and Fluid Flow*, Vol. 28, pp. 211–219, 2007.

63. Bianco, V., O. Manca and S. Nardini, "Numerical Investigation on Nanofluids Turbulent Convection Heat Transfer inside a Circular Tube", *International Journal of Thermal Sciences*, Vol. 50, pp. 341–349, 2011.

64. Behroyan, I., P. Ganesan, S. He and S. Sivasankaran, "Turbulent Forced Convection of Cu–water Nanofluid: CFD Model Comparison", *International Communi-*

cations in Heat and Mass Transfer, Vol. 67, pp. 163–172, 2015.

65. Hejazian, M. and M. K. Moraveji, "A Comparative Analysis of Single and Two-Phase Models of Turbulent Convective Heat Transfer in a Tube for TiO_2 Nanofluid with CFD", *Numerical Heat Transfer, Part A*, Vol. 63, pp. 795–806, 2013.

66. Low, L. K., R. G. Walvekar and S. M. Salim, "CFD Simulation of Forced Convection Nanofluid Flow inside a Circular Conduit", *EURECA*, pp. 57–58, 2013.

67. Esfandiary, M., A. Habibzadeh and H. Sayehvand, "Numerical Study of Single Phase/Two-Phase Models for Nanofluid Forced Convection and Pressure Drop in a Turbulence Pipe Flow", *Journal of Transport Phenomena in Nano-Micro Scale*, Vol. 4, pp. 11–18, 2016.

68. Minea, A. A., "Simulation of Nanofluids Turbulent Forced Convection at High Reynolds Number: A Comparison Study of Thermophysical Properties Influence on Heat Transfer Enhancement", *Flow Turbulence Combust*, Vol. 94, pp. 555–575, 2015.

69. Göktepe, S., K. Atalık and H. Ertürk, "Comparison of Single and Two-phase models for Nanofluid Convection at the Entrance of a Uniformly Heated Tube", *International Journal of Thermal Sciences*, Vol. 80, pp. 83–92, 2014.

70. Fard, M. H., M. N. Esfahany and M. R. Talaie, "Numerical Study of Convective Heat Transfer of Nanofluids in a Circular Tube Two-phase model versus Single-phase Model", *International Communications in Heat and Mass Transfer*, Vol. 37, pp. 91–97, 2010.

71. Kalteh, M., A. Abbassi, M. Saffar-Avval and J. Harting, "Eulerian-Eulerian Two-phase Numerical Simulation of Nanofluid Laminar Forced Convection in a Microchannel", *International Journal of Heat and Fluid Flow*, Vol. 32, pp. 107–116, 2011.

72. Moraveji, M. K. and E. Esmaeili, "Comparison between Single-phase and Two-phases CFD Modeling of Laminar Forced Convection Flow of Nanofluids in a Circular Tube under Constant Heat Flux", *International Communications in Heat and Mass Transfer*, Vol. 39, pp. 1297–1302, 2012.

73. s. Kondaraju and J. S. Lee, "Two-phase Numerical Model for Thermal Conductivity and Convective Heat Transfer in Nanofluids", *Nanoscale Research Letters*, Vol. 6, p. 239, 2011.

74. Murshed, S. M. S., K. C. Leong and C. Yang, "Thermophysical and Electrokinetic Properties of Nanofluids - a Critical Review", *Applied Thermal Engineering*, Vol. 28, pp. 2109–2125, 2008.

75. Davarnejad, R. and M. Jamshidzadeh, "CFD Modeling of Heat Transfer Performance of MgO-water Nanofluid under Turbulent Flow", *Engineering Science and Technology, an International Journal*, Vol. 18, pp. 536–542, 2015.

76. Lotfi, R., Y. Saboohi and A. M. Rashidi, "Numerical Study of Forced Convective Heat Transfer of Nanofluids: Comparison of Different Approaches", *International Communications in Heat and Mass Transfer*, Vol. 37, pp. 74–78, 2010.

77. Miller, A. and D. Gidaspow, "Dense, Vertical Gas-solid Flow in a Pipe", *American Institute of Chemical Engineers Journal*, pp. 1801–1815, 1992.

78. Blasius, P., "Das Aehnlichkeitsgesetz bei Reibungsvorgangen in Flüs sigk eiten", *Forschungsheft*, pp. 1–41, 1913.

79. Rust, J., *Nuclear Power Plant Engineering*, Haralson Publishing Company, Atlanta, Georgia, 1979.

80. Petukhov, B. S., "Heat Transfer and Friction in Turbulent Referred to in Handbook of Single-Phase Convective Pipe Flow with Variable Physical Properties", *Advanced in Heat Transfer*, Vol. 6, pp. 503–565, 1970.

81. Colburn, A. P., "A Method of Correlating Forced Convection Heat Transfer Data and a Comparison with Fluid Friction", *American Institute of Chemical Engineers Journal*, Vol. 29, pp. 174–210, 1933.

82. Manninen, M., V. Taivassalo and S. Kallio, *On the Mixture Model for Multiphase Flow*, VTT Publications, 1996.

83. Schiller, L. and A. Naumann, "A Drag Coefficient Correlation", *Zeitschrift für Acker und Pflanzenbau*, 1935.

84. Kuipers, J., W. Prins and W. V. Swaaij, "Numerical Calculation of Wall to Bed Heat Transfer Coefficients in Gas Fluidized Beds", *American Institute of Chemical Engineers Journal*, pp. 1079–1091, 1992.

85. Whitaker, S., "Forced Convection Heat Transfer Correlations for Flow in Pipes, Past Flat Plates, Single Cylinders, Single Spheres, and for Flow in Packed Beds and Tube Bundles", *American Institute of Chemical Engineers Journal*, pp. 361–371, 1972.

86. Lauder, B. and D. Spalding, *Lectures in Mathematical Models of Turbulence*, Academic Press, London, England, 2010.

87. Ansys, *Fluent 12.0 User's Guide*, 2009.

APPENDIX A: UDF CODES

A.1. Sample UDF Code (Patel *et al.*'s Model)

The Sample UDF Code for Patel *et al.*'s Thermal Conductivity Model:

```
#include "udf.h"

/******thermal cond***/

#define KP 46 % thermal condctivity of solid particles

#define FI 0.00054 % volume concentration

#define KF 0.653 % thermal condctivity of base fluid at bulk temperature

#define CPF 4183.85 % specific heat of base fluid at bulk temperature

#define KB 1.3807e-23 % Boltzmann constant

#define ROF 983.8 % density of base fluid at bulk temperature

#define DP 20e-09 % particle size of solid particles (m)

#define DF 2.75e-10 % particle size of liquid particles (m)

#define A 2.41e-05 % constant

#define B 247.8 % constant

#define C 140 % constant
```

```
DEFINE_PROPERTY(nanofluid_Conductivity,c,t)

{

real pec;

real re;

real k_nf;

real temp = C_T(c,t);

real viscwat;

viscwat =A * pow(10,(B/(temp-C))) ;

pec=((2*KB*temp*ROF*CPF*DP)/(3.14*viscwat*(pow(DP,2))*KF));

k_nf = KF*(1+((DF/DP)*(FI/(1-FI))*(KP/KF)*(1+25000*pec)));

return k_nf;

}
```

A.2. Sample UDF Code (Chon *et al.*'s Model)

The Sample UDF Code for Chon *et al.*'s Thermal Conductivity Model:

```
#include "udf.h"

/******thermal cond***/

#define KP 46 % thermal condctivity of solid particles

#define FI 0.00135 % volume concentration

#define KF 0.61032 % thermal condctivity of base fluid at bulk temperature

#define CPF 4180.6 % specific heat of base fluid at bulk temperature

#define KB 1.3807e-23 % Boltzmann constant

#define LND 1.7e-10 % Mean free path of liquid molecule

#define ROF 996.56 % density of base fluid at bulk temperature

#define DP 50e-09 % particle size of solid particles (m)

#define DF 2.75e-10 % particle size of liquid particles (m)

#define A 2.41e-05 % constant

#define B 247.8 % constant

#define C 140 % constant
```

```
DEFINE_PROPERTY(nanofluid_Conductivity,c,t)

{

real viscwat;

real re;

real k_nf;

real temp = C_T(c,t);

        viscwat = A * pow(10,(B/(temp-C))) ;

        re = (ROF * KB * temp) / (3 * 3.14 * viscwat * viscwat * LND) ;

k_nf = (1 + 64.7 * pow(FI,0.746) * pow((DF/DP),0.369) * pow((KP/KF),0.7476) *
pow((CPF * viscwat/KF),0.9955) * pow(re,1.2321)) * KF;

return k_nf;

}
```